Endothelin Receptor Heterodimerization Inhibits β-arrestin Function

By

Adel Zrein

Submitted in partial fulfillment of the requirements
for the degree of Master of Science

At

Dalhousie University
Halifax, Nova-Scotia
August 2016

Table of Contents

List of Tables

List of Figures

Abstract

Dimerization of G-protein coupled receptors (GPCRs) can affect receptor dynamics at many stages of the GPCR life cycle. Endothelin receptors A (ET_A) and B (ET_B) are co-expressed in vascular smooth muscle cells, and are key to microvascular autoregulation through paracrine signalling following local release of endothelin (ET-1) by endothelial cells. Heterodimerization between ET_A and ET_B prolongs downstream signalling. We hypothesized in this study that endothelin receptor heterodimerization inhibits β-arrestin function, an important mediator in GPCR desensitization, thereby leading to temporal changes in signaling. Using $BRET^2$ technology, the ET_B homodimer and ET_A/ET_B heterodimer were found to form high affinity interactions, while ET_A homodimerization did not occur. The heterodimer reduced and delayed recruitment of β-arrestin-2, and inhibited β-arrestin-1-dependent ERK signalling as assayed with In-Cell Western®. Thus, this study provides novel insights into how endothelin receptor heterodimerization could be affecting the physiological response to ET-1 in tissues co-expressing both receptor subtypes.

List of Abbreviations Used

AT1AR	Angiotensin II receptor type 1
BAD	Bcl-2-Associated Death Promoter
β-arr -	β-arrestin-1 dominant negative (Val-53ΔAsp)
$BRET^2$	Bioluminescence Resonant Energy $Transfer^2$
$BRET_{EFF}$	Bioluminescence Resonant Energy Transfer Efficiency
$BRET_{MAX}$	BRET Maximum
$BRET_{MIN}$	BRET Minimum
cAMP	Cyclic Adenosine Monophosphate
cGMP	Cyclic Guanosine Monophosphate
DMEM	Dulbecco's Modified Eagle's Medium
ECE	Endothelin Converting Enzyme
EGFR	Epidermal Growth Factor Receptor
eIF4e	Eukaryotic Translation Initiation Factor 4E
eNOS	Endothelial Nitric Oxide Synthase
ET-1	Endothelin-1
ET_A	Endothelin receptor A
ET_B	Endothelin receptor B
ER	Endoplasmic Reticulum
ERK	Extracellular-signal Regulated Kinase
FBS	Fetal Bovine Serum
FRET	Fluorescent Resonant Energy Transfer
$GABA_B$	*gamma*-Aminobutyric Acid Receptor B
GAP	GTPase-Activating Protein
GDP	Guanosine Diphosphate
GFP^2	Green Fluorescent $Protein^2$
GPCR	G-Protein Coupled Receptor

GRK	G-protein coupled Receptor Kinase
GTP	Guanosine Triphosphate
HEK293	Human Embryonic Kidney 293 cell line
HERG	Human *ether-a-go-go* related gene
IgG	Immunoglobulin G
IR	Infrared
JNK	c-Jun N-terminal Kinase
LB	Lysogeny Broth
MAPK	Mitogen-Activated Protein Kinase
Mnk1	MAPK-interacting protein kinase 1
NO	Nitric Oxide
PBS	Phosphate-Buffered Saline
PCR	Polymerase Chain-Reaction
PKB	Protein Kinase B
PKC	Protein Kinase C
PLC	Phospholipase C
PTx	*Pertussis* Toxin
Rho	Ras Homolog Gene
RhoGEF	RhoGTPase Nucleotide Exchange Factor
Rluc	*Renilla* luciferase
Taq	*Thermus aquaticus*
VSMC	Vascular Smooth Muscle Cell

Acknowledgements

After two full years of scientific and personal progression, it pleases me to write a brief note thanking those that have aided me along the way. For patiently training me throughout my project, I thank all the current and past members of the labs I've been fortunate enough to work with. I am particularly gracious towards my supervisors Dr. Melanie Kelly and Dr. Eileen Denovan-Wright for allowing me the opportunity to complete this project, as well as for all the overall life mentorship they project towards their students. I can attest that both Dr. Kelly and Dr. Denovan-Wright exemplify the high standard of professionalism and intellect ideally suited to academia. I also want to thank my family and girlfriends for supporting me throughout my stay in Halifax, thank you.

Chapter 1: Introduction

1.1 *G-Protein Coupled Receptors*

G-protein coupled receptors (GPCRs) are a large and diverse family of receptors, sensing various stimuli including hormones, ions, small organic molecules, pressure, and even photons. They share a common architecture formed by seven interconnected transmembrane helices, an extracellular N-terminus and an intracellular C-terminus (Granier and Kobilka, 2012). GPCRs are subdivided based on differences in ligand binding into five major families including Family A, B, C, Adhesion and Frizzled (Fig. 1.1; Culhane *et al.*, 2015).

Agonist activation of a GPCR induces conformational changes within regions of the receptor, which ultimately transduces a signal within the cell, setting off a cascade of events that lead to alterations in cellular function (Katritch *et al.*, 2013). GPCRs directly couple to heterotrimeric guanosine triphosphate (GTP) binding proteins (G-proteins), composed of α, β and γ subunits. Agonist-induced conformational changes in the GPCR serve to increase the affinity of the G-protein to the receptor, and the G-protein subsequently exchanges its bound guanosine diphosphate (GDP) for GTP and becomes activated. Although the sequence of events thereafter remains obscure, binding of GTP is thought to induce conformational changes or dissociation between G-protein α and βγ dimer components (Preininger *et al.*, 2013), each of which goes on to activate distinct downstream effectors (Oldham and Hamm, 2008). The GTP-bound Gα subunit is inactivated by intrinsic hydrolytic activity, returning to its inactive GDP-bound state (Chen and Manning, 2001).

Figure 1.1: *Comparison of GPCR family groups*

Family A GPCRs bind a wide range of diverse ligands in the transmembrane region and have a short N-terminus. Family B GPCRs bind larger peptide hormones in their long extracellular N-terminus. Family C receptors have large extracellular N-terminal ligand-binding region in the “Venus flytrap” fold for ligand binding with a conserved disulfide linkage to constitutively form dimers (Zhang *et al.*, 2014). The Adhesion and Frizzled families have GPCR-like transmembrane-spanning regions fused together with one or several functional N-terminal domains. Adhesion families contain auto-proteolytic domains and will cleave their N-terminus following ligand activation, while Frizzled receptors are activated by Wnt proteins. Ligands are shown in red and listed above each family group.

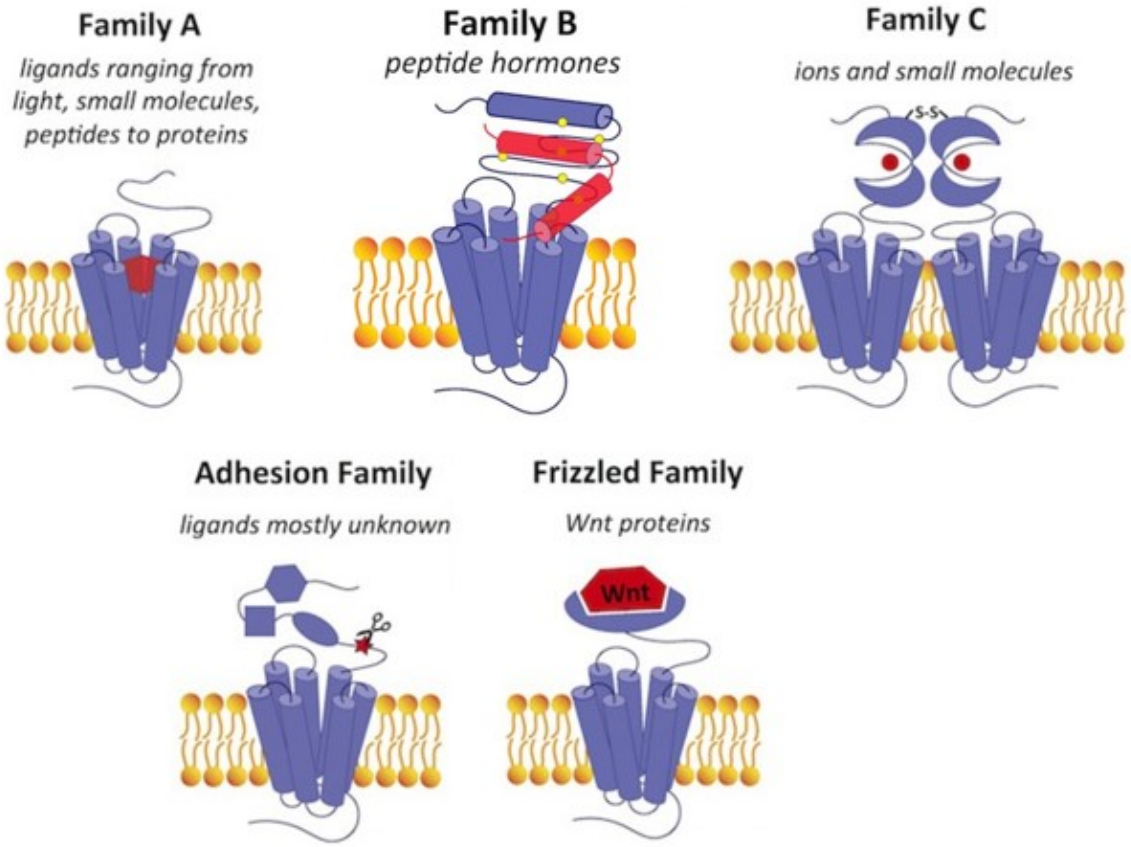
Family A
ligands ranging from light, small molecules, peptides to proteins
Family B
peptide hormones
Family C
ions and small molecules
S-S
Adhesion Family
ligands mostly unknown
Frizzled Family
Wnt proteins
Wnt

G-proteins are subdivided into 4 major groupings based on the α subunit sequence similarity: Gαs, Gαi, Gαq and $G\alpha_{12/13}$. These differ functionally by the set of downstream effectors each α-subunit couples with following ligand binding and GPCR activation. Gαs will activate the enzyme adenylate cyclase to produce second messenger cyclic adenosine monophosphate (cAMP), Gαi inhibits adenylate cyclase, Gαq activates the enzyme phospholipase C (PLC), to produce second messengers inositol trisphosphate (IP_3) and diacylglycerol (DAG), and $G\alpha_{12/13}$ activates RhoGTPase nucleotide exchange factors (RhoGEFs) to initiate protein phosphorylation cascades (Svoboda *et al.*, 2004; Venkatakrishnan *et al.*, 2013). The production of second messengers allows for amplification of the initial GPCR signal, thus allowing minor stimuli to achieve relatively important cellular effects, commonly via activation of kinase proteins that can phosphorylate a myriad of downstream targets (Fig. 1.2; Martins *et al.*, 2012).

1.2 *β-arrestin in Trafficking and Signaling*

GPCRs that are activated by ligand may terminate their signaling through several mechanisms. GTP-bound G-proteins are inactivated by intrinsic hydrolysis of GTP to GDP, a reaction accelerated by GTPase-Activating Proteins (GAPs; Ross, 2013). Parallel to the above, agonist-induced conformational changes in GPCRs promotes rapid recruitment of G-protein coupled receptor kinases (GRKs) which phosphorylate serine/threonine residues within the intracellular loop 3 or C-terminus of the GPCR. This serves as an anchor for recruitment of β-arrestin, which sterically hinders G-protein recruitment, thus desensitizing the GPCRs to the initial stimuli (Smith and Rajagopal, 2016).

Figure 1.2: *G protein-coupled receptor activation and regulation*

(A) GPCR activation enables the exchange of GDP to GTP by the α subunit of the G-protein. (B) The GTP-bound α subunit then activates an effector such as phospholipase C (PLC). (C) Second messenger molecules like inositol-1,4,5-triphosphate (IP_3), which opens calcium channels present on the endoplasmic reticulum (ER) and initiates Ca^{2+} release, are direct products of enzymatic conversion. (D) G protein-coupled receptor kinases (GRKs) phosphorylate intracellular regions of the GPCR. (E) β-arrestins can recognize the phosphorylated GPCR and trigger internalization, leading to receptor degradation or recycling to the plasma membrane. (F) Second messenger molecules and β-arrestin-mediated MAPK cascades, such as ERK activation, lead to downstream biological events, frequently regulation of gene expression.

Reproduced and modified with permission from *Trends in Biotechnology* (Martins *et al.*, 2012; see Appendix I for license).

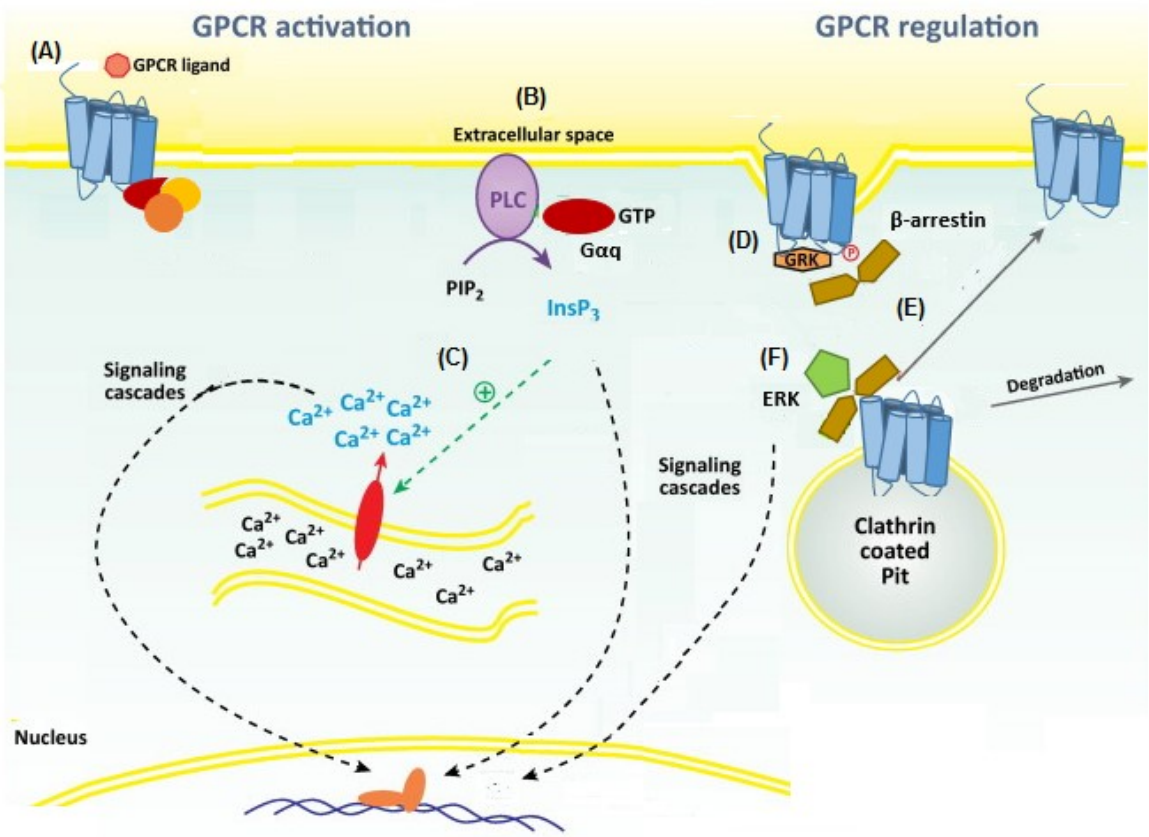
GPCR activation
GPCR regulation
(A)
GPCR ligand
(B)
Extracellular space
PLC
GTP
Gαq
PIP2
InsP3
(C)
Signaling cascades
Ca2+
(D)
GRK
β-arrestin
(E)
(F)
ERK
Degradation
Signaling cascades
Clathrin coated Pit
Nucleus

β-arrestin further serves as a scaffold protein, allowing for the formation of clathrin-coated caveolae and endocytosis of the GPCR complex. The GPCR may then be recycled to the plasma membrane, or targeted to lysosomes for degradation (Luttrell *et al.*, 2002; Gainetdinov *et al.*, 2004).

There are four arrestin isoforms in rodents and humans: two of which are exclusively expressed in photoreceptor cells (Moaven *et al.*, 2013), while the two others, termed β-arrestin-1 and β-arrestin-2, are expressed in virtually all tissue types (Pierce and Lefkowitz, 2001). Murine knock-out of either β-arrestin 1 or 2 isoform produces viable offspring, whereas double knock-out of both isoforms is embryonically lethal, indicating that there is sufficient overlap in β-arrestins biological functions to compensate for loss of one isoform and collectively their function is essential for survival (Conner *et al.* 1997; Kohout *et al.*, 2001). Certain GPCRs possess differential affinities to β-arrestin 1 or 2, leading to internalization that is more reliant on one isoform over the other; as is the case with the predominantly β-arrestin-2 dependent internalization of the β_2 adrenergic receptor (Oakley *et al.*, 2000).

In addition to the primary roles of β-arrestins in GPCR signal attenuation and receptor downregulation, β-arrestins also initiate signaling cascades of their own (Lefkowitz and Shenoy, 2005). In effect, β-arrestins are downstream effectors of G-protein-independent GPCR signaling. The most studied β-arrestin- 1 and 2 signaling pathway involves the direct and indirect binding of serine/threonine/tyrosine kinases referred to as mitogen-activated protein kinases (MAPKs). MAPKs are part of a chain of kinase proteins that regulate numerous

transcription factors, ultimately affecting gene expression in the nucleus to promote progression through the cell cycle and cellular proliferation (Pearson *et al.*, 2001). Multiple MAPK family members have been shown to interact with β-arrestin- 1 and 2, such as extracellular receptor-regulated kinase 1/2 (ERK 1/2; Tohgo *et al.,* 2002; Shenoy *et al.*, 2006), p38 kinases (Bruchas *et al.*, 2006), and the c-Jun N-terminal kinases (JNKs; McDonald *et al.*, 2000).

Initiation of MAPK cascades downstream of GPCR activation is the result of numerous downstream effectors differing with respect to temporal and spatial patterns. For example, agonist activation of the Gαq-coupled angiotensin II receptor type 1 (AT1AR) initiates a rapid and transient G-protein-dependent ERK phosphorylation that is quickly quenched by endogenous β-arrestin-mediated desensitization or altogether eliminated by inhibition of protein kinase C (PKC). Parallel to the transient G-protein-dependent ERK signalling, β-arrestin-dependent ERK phosphorylation develops slowly yet lasts for over an hour due to the long-lasting association between AT1AR and β-arrestin (DeWire *et al.*, 2007).

As β-arrestin scaffolding is trafficked to endosomal vesicles following GPCR internalization, its MAPK cascade activation is spatially restrained to specific cellular locations (Luttrell *et al.*, 2001; Ahn *et al.*, 2004). The functional implications of β-arrestin-mediated ERK phosphorylation are increasingly being described. Phosphorylated ERK appears to remain bound to β-arrestin in the cytosol and not enter the nucleus, inhibiting the usual ERK-dependent transcription of Elk-1, a transcription factor involved in the transcription of genes that promote cell cycle progression (Tohgo *et al.*, 2002). β-arrestin-mediated AT1AR-ERK signaling

blocks apoptosis through phosphorylation of pro-apoptotic Bcl-2-associated death promoter (BAD) (Ahn et al., 2009), stimulates translation through MAPK-interacting protein kinase 1 (Mnk1) phosphorylation of eukaryotic translation initiation factor 4E (eIF4e) (DeWire et al., 2008), and initiates S-phase entry and cellular proliferation via epidermal growth factor receptor (EGFR) (Kim et al., 2009), supporting that β-arrestin-dependent ERK signaling regulates numerous important developmental processes.

1.3 *GPCR Dimerization*

The classical model that GPCRs act as single monomeric entities has been challenged by contemporary literature (Bouvier and Hebert, 2014; Milligan, 2007). There is no debate that many isolated GPCRs are capable of coupling to and activating downstream effectors as monomers (Whorton *et al.*, 2007), but a growing body of research indicates this is not the only physiological condition under which GPCRs operate. Dozens of independent studies have provided evidence of dimerization of GPCRs, along with the importance of such interactions to downstream signaling. In many cases, GPCR dimerization is constitutive, beginning in the endoplasmic reticulum (ER) before exportation to the plasma membrane, and continuing until eventual internalization and lysosomal degradation (Dupré *et al.*, 2006; Harding *et al.*, 2009).

GPCR dimerization can exert functional consequences at many stages of the GPCR life-cycle (Fig. 1.3). It can affect biosynthesis of GPCRs; the most striking example of this is the gamma-aminobutyric acid B receptor ($GABA_B$), which must form homodimers or heterodimers comprised of $GABA_{B1}$ and $GABA_{B2}$

subunits within the ER to be exported to the plasma membrane (Kaupmann *et al.*, 1998; Villemure *et al.*, 2005; Richer *et al.*, 2009). Physical interactions between GPCRs have also been demonstrated to modulate pharmacological aspects of ligand behaviour such as positive or negative cooperativity (changes in ligand affinity) and signaling bias (Terrillon and Bouvier, 2004). Dimerization of GPCRs may also potentiate, attenuate, or even bias downstream coupling of the receptors. For example, co-activation of both the dopamine receptor 2 (D_2) and type 1 cannabinoid receptor (CB_1) switches the signaling of CB_1 from Gαi to Gαs; this is thought to be mediated by allosteric modulation of CB_1 conformation by the physically interacting D_2 (Bagher *et al.*, 2016). Dimerization of GPCRs can also affect trafficking behaviours such as co-internalization along a common pathway: co-internalization of the A_{2A} adenosine/D_2 dopamine heterodimer is observed following agonist activation of D_2 (Hillion et al, 2002). Although evidence of dimerization exists for a large number of GPCRs, the implications of these interactions are only beginning to be unravelled and have functional consequences in health and disease as well as future drug design campaigns targeting these receptors. Identifying ligands capable of selectively binding to and regulating GPCR heterodimers is proposed as a means of increasing the specificity and decreasing off-target effects of clinical pharmacological interventions, and is an emerging area of research (Daniels *et al.* 2005; Eglen et al., 2007; Dalrymple et al., 2008; Glass *et al.*, 2016).

Figure 1.3: *Potential functions of GPCR dimerization*

(1) Dimerization has been shown to have a primary role in maturation and transport of certain GPCRs from the endoplasmic reticulum (ER) to the cell surface. (2) GPCR heterodimerization can lead to both positive (+) and negative (−) ligand binding cooperativity, as well as (3) potentiating (+) or attenuating (−) signaling or biasing G-protein selectivity. (4) Heterodimerization can promote (+) or inhibit (-) co-internalization of two receptors after the stimulation of only one protomer. G: G protein; L: ligand.

Reproduced and modified with permission from *EMBO Rep*. (Terrillon and Bouvier 2004; see Appendix II for license).

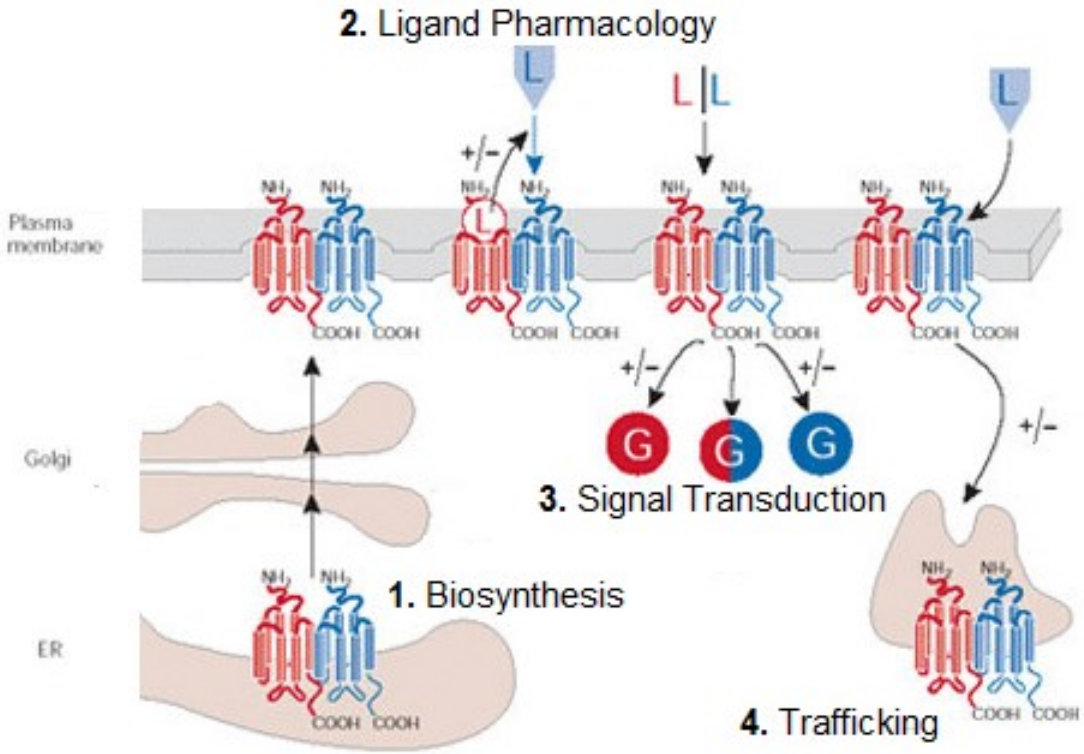
2. Ligand Pharmacology
L
L L
L
+/-
Plasma membrane
COOH COOH
+/-
+/-
+/-
G
G
G
3. Signal Transduction
Golgi
1. Biosynthesis
ER
4. Trafficking

1.4 *The Endothelin System*

The endothelin system is comprised of endothelin receptors A (ET_A) and B (ET_B), in addition to three endogenous peptide activators termed endothelin 1-3 (ET-1/ET-2/ET-3). ET-1 is the most studied endothelin isoform and, along with ET-2, is non-selective in its capacity to activate ET_A and ET_B, whereas ET-3 is highly selective towards ET_B (Ling *et al.*, 2013). The endothelin system contributes to several key physiological processes including basal vascular and lung airway tone, cardiac inotropy and chronotropy, renal sodium and water balance, central nervous system hormone release, and cellular proliferation (Maguire and Davenport, 2014). In endothelial cells, ET-1 mRNA is translated into a precursor protein that is processed by proteases, including isoforms of endothelin converting enzymes (ECE) to yield bioactive ET-1 (Kido *et al.*, 1998; D'Orléans-Juste *et al.*, 2003). In vasculature, ET-1 is stored in Weibel-Palade bodies within endothelial cells and released constitutively to regulate basal vascular tone, or dynamically in response shear stress to regulate arteriole vascular tone following variations in systolic pressures, allowing the endothelin system to autonomously function locally (Vozzi *et al.*, 2014). Thus, the endothelin system contributes to organ blood flow and peripheral vascular resistance. ET-1 is also released in response to cytokines, angiotensin, vasopressin, and oxygen free radicals (Emori *et al.*, 1991). Upon binding ET-1, ET_A is rapidly internalized and recycled to the plasma membrane, whereas ET_B along with its bound ET-1 is directed to lysosomal degradation, thus also clearing locally produced ET-1 (Bremnes *et al.,* 2000).

Although ET-1 is an extremely potent and long-lasting vasoconstrictor, it also signals to mediate vasodilation. This dual action is explained by the expression of ET_B on endothelial cells and co-expression of ET_A and ET_B on vascular smooth muscle cells (VSMC) (Fig. 1.4). Activation of both ET_A or ET_B leads to Gαq-dependent production of second messengers IP_3 and DAG by PLC. IP_3 diffuses to the ER and opens ligand-gated Ca^{2+} channels, increasing cytosolic Ca^{2+} levels. In endothelial cells, ET_B-mediated Ca^{2+} release activates endothelial nitric oxide synthase (eNOS) to produce short-lived nitric oxide (NO), which diffuses to adjacent VSMCs and activates VSMC soluble guanylate cyclase to produce cyclic guanosine monophosphate (cGMP). cGMP promotes vasodilation mainly through activation of K^+ channels, culminating in a hyperpolarized VSMC membrane potential (Carvajal *et al.*, 2000). Endothelial ET_B activation also releases vasodilating prostacyclin and endothelium-derived hyperpolarizing factor (Mazzuca and Khalil, 2012).

In VSMCs, endothelin-mediated Ca^{2+} release following activation of ET_A and ET_B promotes calmodulin to phosphorylate myosin light chain kinase, enabling it to phosphorylate the light chain myosin and allow cross-bridging between actin and myosin filaments, leading to vasoconstriction. The process of smooth muscle relaxation is initiated by dephosphorylation of light chain myosin by myosin phosphatase (Webb, 2003) and cell hyperpolarization via Ca^{2+}-sensitive K^+ channels (Petkov, 2012).

Figure 1.4: *Vascular endothelin system*

Endothelial ET-1 release is controlled via regulation of gene transcription and ECE activity. ET-1 acts as a local paracrine factor on smooth muscle ET_A and ET_B receptors to induce vasoconstriction and mitogenesis. ET-1 also acts in an autocrine manner at endothelial cell ET_B receptors to stimulate vasorelaxation via release of nitric oxide (NO) following activation of endothelial nitric oxide synthase (eNOS). ET_B receptors also clear local ET-1 by degradation following ET_B internalization.

Modified from *Clinical Science* (Tostes *et al.*, 2008).

Blood flow

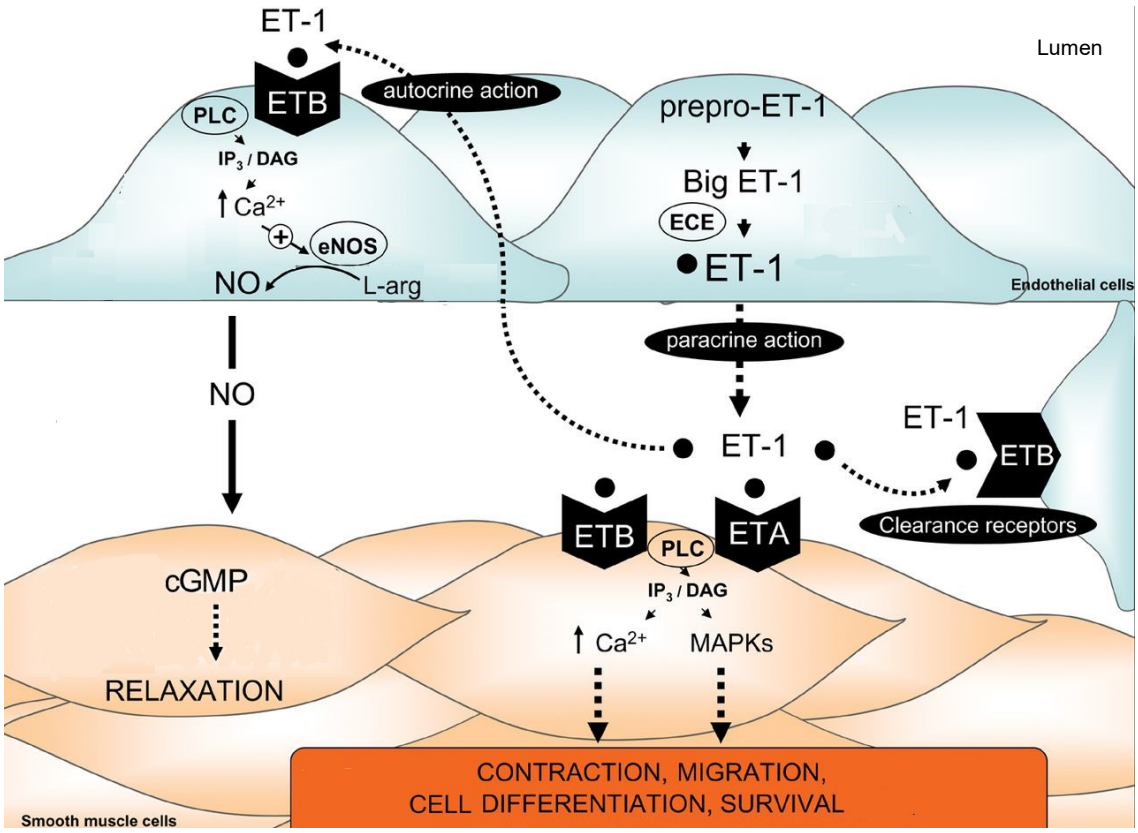
ET-1
Lumen
ETB
autocrine action
PLC
IP3 / DAG
↑ Ca2+
eNOS
NO
L-arg
prepro-ET-1
Big ET-1
ECE
ET-1
Endothelial cells
paracrine action
NO
ET-1
ET-1
ETB
Clearance receptors
ETB
PLC
ETA
IP3 / DAG
cGMP
↑ Ca2+
MAPKs
RELAXATION
CONTRACTION, MIGRATION,
CELL DIFFERENTIATION, SURVIVAL
Smooth muscle cells

1.5 Endothelin Receptor Dimerization

Like many other Family A GPCRs (Hiller *et al.*, 2013), endothelin receptors homodimerize and heterodimerize (Gregan *et al.,* 2004; Evans and Walker, 2008). Studies supporting this have used techniques such as co-immunoprecipitation and Fluorescent Resonant Energy Transfer (FRET). Experimentation utilizing heterologous expression in cell culture provides compelling evidence that dimerization between ET_A and ET_B alters important receptor signaling characteristics.

Evidence to date suggests that endothelin receptor heterodimerization delays desensitization and prolongs G-protein-dependent signaling. HEK293 expressing either ET_A or ET_B rapidly desensitize ($t_{1/2}$ < 1 minute) following ET-1 exposure, whereas HEK293 cells co-expressing both receptor subtypes fail to desensitize (Dai and Galligan, 2006). Evans and Walker (2008) later corroborated this finding; reporting prolonged Ca^{2+} transients in HEK293 cells co-expressing both ET_A and ET_B versus the expression of a single receptor subtype. They further demonstrated that expressing mutant ET_A receptor that is non-dimerizing but nonetheless functional in its capacity to generate Ca^{2+} transients abolishes this effect; indicating that the observed Ca^{2+} transient prolongation is heterodimer-dependent. ET-1 binding to ET_A is quasi-permanent, with only 40% dissociation after 4 hours (Devesly *et al.*, 1990), and thus internalization and desensitization are essential mechanisms towards attenuation of endothelin signaling. Thus, heterodimer-dependent alterations of these processes would likely significantly affect the time available for ET-1 to exert its effect.

It remains to be seen if the aforementioned *in vitro* observations translate to tissues co-expressing both endothelin receptor sub-types. If so, heterodimerization of endothelin receptors could partially explain the extraordinarily long vasopressor human response to ET-1, on the order of one to two hours (Clarke *et al.*, 1989; Macrae *et al.*, 1993). Selective inhibition of endothelin receptor heterodimers could provide a means increasing the specificity of endothelin antagonists by solely targeting tissues co-expressing both receptor subtypes.

1.6 Hypothesis and Objectives

The functional consequences of endothelin receptor heterodimerization, namely prolongation of Ca^{2+} transients, could potentially be explained by a failure of β-arrestin and subsequent internalization machinery to properly recognize and attenuate the activated endothelin receptor heterodimers. If this hypothesis is tenable, the heterodimers reduced ability to recruit internalization machinery should concomitantly decrease the extent of β-arrestin-dependent signaling such as ERK phosphorylation.

The hypothesis of this thesis is that endothelin receptor heterodimerization inhibits β-arrestin recruitment and β-arrestin-dependent signaling.

Specific objectives include:

1. Quantify the affinity of endothelin receptors to form dimers
2. Determine if heterodimerization affects the recruitment of β-arrestin 1 or 2
3. Determine if heterodimerization affects β-arrestin dependent signaling

Chapter 2: Methods and Reagents

***2.1** Generation of Constructs*

ET_A and ET_B mammalian expression vectors were generated with either green fluorescent protein^2 (GFP^2) or *Renilla* luciferase (Rluc) genes in frame at the 3' termini. Human ET_A and ET_B receptor sequences were obtained by polymerase chain-reaction (PCR) with *Thermus aquaticus* (Taq) polymerase (Invitrogen Canada Inc.) using 3x N-terminus HA-tagged ET_A or N-terminus Myc-tagged ET_B templates (SinoBiological) (primers in Table 2.1). Primers were designed to remove stop codons and incorporate *PstI* (5') and *HindIII* (3') restriction sites.

PCR products were electrophoresed on a 0.8% (w/v) agarose gel and visualized with a UV transilluminator; bands were cut out and DNA purified using the GenElute DNA Extraction kit (Sigma-Aldrich) and then ligated into pGEM-T Easy vector (Promega) with T4 DNA ligase. The resulting constructs were transformed into chemocompetent *E. coli* and plated on X-gal coated agar plates containing 50 µg/mL ampicillin followed by an overnight incubation at 37 ^oC. White colonies were selected for further overnight incubation in Lysogeny broth (LB) broth containing 50 µg/mL ampicillin. Plasmid DNA was extracted from the transformed *E. coli* using the GenElute Plasmid Miniprep kit (Sigma-Aldrich). The generated ET_A-pGEM-T Easy, ET_B-pGEM-T Easy, as well as $pGFP^2$-N3 and pRluc-N1 plasmids (Perkin-Elmer) were all double digested using *PstI* and *HindIII*, and digestion reactions were run on a 0.8% agarose gel. DNA products of interest were isolated, and the digested ET_A and ET_B sequences were each ligated into both $pGFP^2$-N3 and pRluc-N1 plasmids. These constructs were then transformed into chemocompetent *E. coli* and ET_A/ET_B -$pGFP^2$-N3 transformed cells were plated on

agar plates containing 25 µg/mL zeocin, while ET_A/ET_B-pRluc-N1 transformed cells were plated on agar plates containing 25 µg/mL kanamycin to select for transformed colonies. Resulting colonies were further cultured in 25 µg/mL kanamycin LB broth, and plasmid DNA extracted using the GenElute Plasmid Miniprep kit. All receptor sequences were confirmed by Sanger sequencing (GENEWIZ Inc.).

Human β-arrestin-2-pGEM-T vector (SinoBiological) was processed using similar methodology to produce β-arrestin-2-GFP^2 (primers in Table 2.1). The carboxy-terminus GFP^2 fusion construct of human *ether-a-go-go* related gene (HERG-GFP^2) and the Rluc-GFP^2 fusion construct were kindly provided by Dr. Terry Hebert (McGill U., Montreal). The β-arrestin-1 dominant negative (Val-53ΔAsp) and the human β-arrestin-1-GFP^2 pcDNA3.1 plasmids were provided by Dr. Eileen Denovan-Wright (Dalhousie U., Halifax), and previously described in Ferguson *et al.*, 1996 and Laprairie *et al.*, 2014, respectively.

2.2 *Cell Culture*

Human embryonic kidney (HEK) 293 cells (Invitrogen) were maintained in Dulbecco's Modified Eagle's Medium supplemented with 10% fetal bovine serum (DMEM, FBS; Thermo Fisher Scientific) inside sealed flasks (Corning) at 37 ºC in a 5% CO_2 environment. Cells were subcultured (1:10) when they reached 90-100% confluency by aspirating media and incubating in trypsin for 3 minutes. DMEM was then added to inactivate the trypsin, and the cells were transferred to a 15 mL conical tube and spun at x 400 g for 3 minutes. The cell pellet was resuspended in fresh DMEM and used for passaging and plating for experiments.

Table 2.1: *Oligonucleotides used to generate fusion constructs*

Construct	Primer (5' to 3')
ET_A-Rluc and ET_A-GFP^2	Sense AACTGCAGATGGAAACCCTTTGCCTC Antisense CCCAAGCTTGTTCATGCTGTCCTTATG
ET_B-Rluc and ET_B-GFP^2	Sense AACTGCAGATGCAGCCGCCTCCAAGT Antisense CCCAAGCTTAGATGAGCTGTATTTATT
β-arrestin-2-GFP^2	Sense ATATGAATTCATGGGGGAGAAACCC Antisense ATATAAGCTTTCCGCAGAGTTGATCATC

2.3 *Cell Transfection*

All transfections were carried out using Lipofectamine 2000 cationic lipid transfection reagent (Invitrogen Inc.) (Dalby *et al.*, 2004). Briefly, 7 µL of Lipofectamine reagent and 4 µg of plasmid DNA were each diluted separately in 250 µL Opti-MEM (Thermo Fisher Scientific) and vigorously mixed followed by a 10-minute incubation at room temperature. The Lipofectamine and DNA were then combined and allowed to incubate together for 20 minutes at room-temperature. Plasmid DNA was supplemented with empty pcDNA 3.1+ vector to achieve 4 µg total DNA in all transfections. The resulting transfection mix was then added to >75% confluent HEK293 cells growing in 6-well plates (Corning) containing serum-free DMEM. Plates were then incubated for 48 hours before experimentation, or resuspended 24 hours later and aliquoted into a clear 96-well plate (Corning) for In-Cell Western® (see below), followed by another 24-hour incubation.

2.4 *Bioluminescence Resonance Energy Transfer^2 (BRET^2)*

The BRET^2 method was used to assay for endothelin receptor physical interactions or β-arrestin recruitment (See Fig. 2.1). BRET^2 utilizes a unique Rluc substrate, DeepBlueC coelenterazine (PerkinElmer) which emits light between 290-400 nm during the Rluc-mediated oxidation reaction. If the Rluc protein is in close proximity (50-100 Å) to a molecule of GFP^2, then there is resonance energy transfer to the GFP^2, exciting it to emit at 505-508 nm (Ramsay *et al.*, 2002). BRET^2 provides an advantage over previous resonance energy transfer techniques in that there is greater spectral resolution between Rluc and GFP^2 emission wavelengths, which reduces the amount of background signal.

Transfected HEK293 cells plated in a 6-well plate were first resuspended in 1 mL of BRET buffer which was made by supplementing 50 mL of PBS with 1.0 g/L glucose, and 2 Mini Complete ULTRA protease inhibitor cocktail tablets (Roche, Mannheim, Germany) then spun at x 400 g for 1 minute. The cell pellet was resuspended in BRET buffer and 90 µL was then dispensed into a white 96 well plate (Perkin-Elmer). BRET was measured with a Luminoskan Ascent plate reader (Thermo Scientific, Waltham, MA) immediately after adding DeepBlueC coelenterazine substrate to a final concentration of 5 µM. All measurements were conducted with the plate reader set to make dual luminescent emission measurements with 510 and 405 nm filters, with the integration time set to 10 s, and the photomultiplier tube voltage set to 1200. Raw 510/405 emission ratios were then converted to BRET efficiency ($BRET_{EFF}$) by subtracting the minimum obtainable emission ratio ($BRET_{MIN}$) and dividing this sum by the maximum obtainable emission ratio ($BRET_{MAX}$), by utilizing Rluc transfected cells as the minimum ratio, and Rluc-GFP^2 fusion construct transfected cells as the maximum obtainable ratio (equation 1, see page 28).

BRET saturation curves were carried out to demonstrate the specificity of an interaction. In such experiments, a fixed amount of Rluc-fusion construct is co-transfected with increasing amounts of GFP^2-fusion construct. $BRET_{EFF}$ is then plotted against the mass ratio of GFP^2/Rluc plasmid used during transfection. A specific interaction is demonstrated by a plateau in the increase of $BRET_{EFF}$ over the range GFP^2/Rluc transfection ratios used.

Figure 2.1: *Principles of Bioluminescence Resonance Energy Transfer*[2]

A. Proteins that do not form physical interactions, in this case GPCRs, are expressed in frame with Rluc or GFP[2]. On the left hand, when the Rluc tag oxidizes the DeepBlueC coelenterazine substrate and emits a blue light, the GFP[2] tag is not in close enough proximity to be excited into emitting. On the right panel is the emission profile spectrum for co-expressed but non-interacting Rluc and GFP[2], with a peak at ~400 nm corresponding to Rluc emission. **B.** Physically interacting proteins of interest, in this case GPCRs, are expressed in frame with Rluc or GFP[2]. On the left hand, when the Rluc tag oxidizes the DeepBlueC coelenterazine substrate and emits a blue light, the GFP[2] tag is excited by this wavelength light and, in turn, emits a green light. On the right panel is the emission profile spectrum for co-expressed Rluc and GFP[2] in close proximity, with a peak at ~400 nm corresponding to Rluc emission, and the subsequent peak at ~500 nm corresponding the GFP[2] emission.

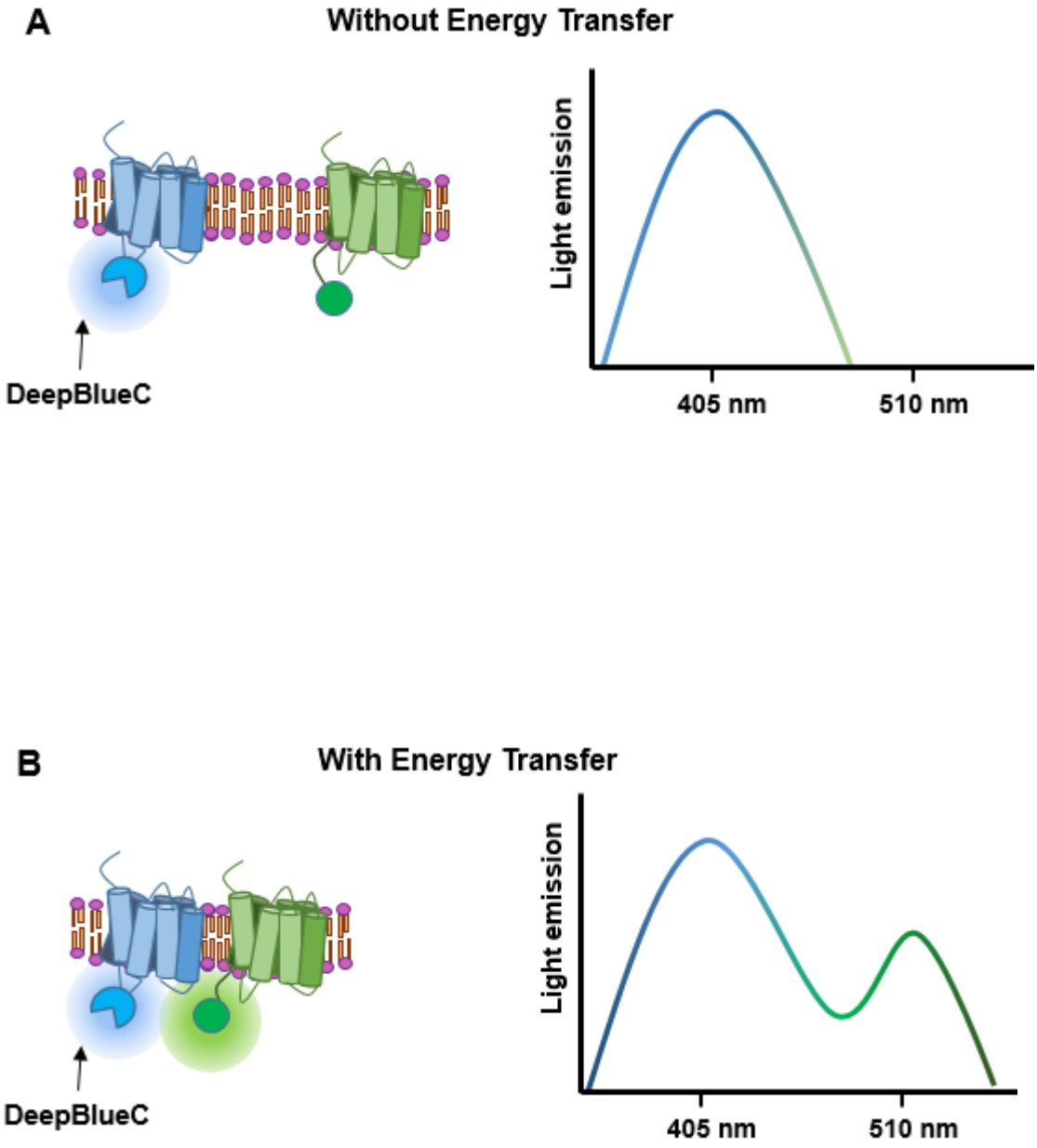
A
Without Energy Transfer
DeepBlueC
Light emission
405 nm
510 nm
B
With Energy Transfer
DeepBlueC
Light emission
405 nm
510 nm

***2.5** In-cell Western®*

In-cell Western® method was used to assay ERK phosphorylation (Lovell *et al.*, 2015). 24 hours after transfection, HEK293 cells in 6-well plates were washed in serum-free DMEM, and each well was resuspended in 1600 µL DMEM. 100 µL was plated per well on poly D-lysine coated clear 96-well plate (Corning). Cells were then allowed to incubate for a further 24 hours. Cells were treated with ET-1 to a final concentration of 10 nM, a dose known to achieve maximal response in cell culture experiments (Yanagisawa *et al.*, 1988; Evans and Walker, 2008). Cells were then fixed for 10 minutes with 4% paraformaldehyde at the selected time-points. Cells were then washed 3 times for 5 minutes in PBS, and permeabilized by shaking at room-temperature for 60 minutes in blocking buffer consisting of 20% Odyssey Blocking Buffer (Li-cor) and 0.3% Triton X-100 (Sigma-Aldrich) diluted in PBS. Primary antibodies rabbit polyclonal IgG against C-14 of ERK 1/2 (Santa Cruz Biotechnology) and goat polyclonal IgG against Tyr-204 of phosphorylated ERK (p-ERK, Santa Cruz Biotechnology) were applied to wells at 1:200 dilutions in blocking buffer and cells were incubated for one hour at room-temperature, followed by over-night incubation at 4 ^{o}C. The following day, wells were washed as described above in PBS and then incubated in secondary antibodies IR-Dye800 conjugated donkey anti-rabbit IgG (Rockland) and Alexa Fluor 680 conjugated donkey anti-goat IgG (Thermo Fisher Scientific), both diluted 1:500 in blocking buffer with shaking for 2 hours at room-temperature. Wells were then washed as above with an additional 5-minute wash in double-distilled H_2O (ddH_2O) and dried over-night. To subtract background auto-emission and non-specific binding, an

additional well from each transfection was treated with the same immuno-blotting procedure, with the exception that primary antibodies were not applied. *Pertussis* toxin dissolved in ddH_2O (PTx, Sigma-Aldrich) was used to inhibit Gαi signalling and was added to the media (0.5 pg/μL) 24 hours prior to drug treatment. Non-selective PKC inhibitor Gö-6983 (Sigma) was applied at the maximal inhibitory concentration of 100 nM (Park *et al.*, 2000), one hour prior to ET-1 treatment.

The relative abundances of p-ERK and total ERK were quantified using the Li-Cor Odyssey Imaging System v3.0, with the read setting set to Microplate 2, the resolution set to 169 μm, quality set to medium, channel 700 (ERK) intensity set to 6 and channel 800 (p-ERK) set to 7.5. A grid was fit to the captured image and the intensities of each well was obtained. Background intensities were subtracted and the ratio of p-ERK to total ERK calculated for each well.

2.6 *Statistical Analysis and Curve Fitting*

All data are presented as the mean ± standard error of the mean. Statistical analyses were performed using Graphpad Prism v.6 (Graphpad Software Inc.). In BRET saturation curve experiments, the data were fit to a rectangular hyperbola (equation 2, page 28), where B_{MAX} is equivalent to $BRET_{MAX}$ and K_d to $BRET_{50}$. In time-course experiments, the data were fit to a variable slope sigmoidal dose-response (equation 3, page 28), where EC_{50} is a measure of the rate of association ($t_{1/2}$). Statistical comparisons between points were done with multiple t-tests corrected for multiple comparisons using the Holm-Sidak method, with significance assumed at $P<0.05$, while statistical comparisons of $BRET_{MAX}$ and time to half-maxima were performed using unpaired two-tailed *t* without post-hoc testing.

Equations:

1. $BRET_{EFF} = (405/510 - BRET_{MIN})/(BRET_{MAX})$
2. *Rectangular hyperbola fit:* $Y = B_{MAX} \times X/K_d + X$
3. *Sigmoidal fit:* $Y = Bottom + (Top - Bottom)/(1 + 10^{(EC50-X)\times Hill\ Slope})$

Chapter 3: Results

3.1 *Physical Interactions Between Endothelin Receptors*

Endothelin receptor dimerization was confirmed by $BRET^2$ in HEK293 cells. BRET efficiency ($BRET_{EFF}$) was measured in cells co-transfected with 1 µg ET_A-Rluc and 2 µg of either ET_A-GFP^2 (n=4), ET_B-GFP^2 (n=4), or HERG-GFP^2 (n=3) (Fig. 3.1A). ET_A-Rluc and ET_A- or ET_B-GFP^2 produced a significantly higher $BRET_{EFF}$ compared to HERG-GFP^2, a membrane protein that does not interact with GPCRs (Bagher *et al.,* 2013). $BRET_{EFF}$ was also measured in cells transfected with 1 µg ET_B-Rluc and 2 µg of either ET_B-GFP^2 (n=4), ET_A-GFP^2 (n=4), or HERG-GFP^2 (n=3) (Fig. 3.1B). The ET_B-Rluc and ET_B-GFP^2 combination had significantly higher $BRET_{EFF}$ over the HERG-GFP^2 control. Thus, the heterodimer was detectable only with ET_A as donor and ET_B as acceptor, which could have been due to different distances or orientations between Rluc and GFP^2 molecules (Pfleger *et al*., 2006).

BRET saturation curves were generated to test if endothelin receptor physical interactions were specific or due to random collision. 1 µg donor was transfected along with increasing amounts of acceptor. If the physical interaction was specific, $BRET_{EFF}$ would eventually plateau when all donor molecules were occupied. The ability of endothelin receptors to form homodimers or heterodimers in HEK293 cells was tested by transfecting HEK293 cells with: 1 µg ET_A-Rluc along with 0-3 µg of either ET_A-GFP^2 (n=4) or HERG-GFP^2 (n=3) (Fig. 3.2), 1 µg ET_B-Rluc along with 0-3 µg of either ET_B-GFP^2 (n=4) or HERG-GFP^2 (n=3) (Fig. 3.3), and 1 µg ET_A-Rluc along with 0-3 µg of either ET_B-GFP^2 (n=4) or HERG-GFP^2 (n=3) (Fig. 3.4). Corresponding $BRET_{MAX}$ and $BRET_{50}$ values are summarized in Table 3.1.

Figure 3.1: *ET_A and ET_B $BRET^2$ constructs produced energy transfer*

A. $BRET_{EFF}$ values obtained from HEK293 cells transiently transfected with 1 µg ET_A-Rluc and 2 µg ET_A- (n=4), ET_B- (n=4), or HERG-GFP^2 (n=3), as indicated. **B.** $BRET_{EFF}$ values obtained from HEK293 cells transiently transfected with 1 µg ET_B-Rluc and 2 µg ET_A- (n=4), ET_B- (n=4), or HERG-GFP^2 (n=3), as indicated.

* $P<0.05$ compared to HERG-GFP^2 control.

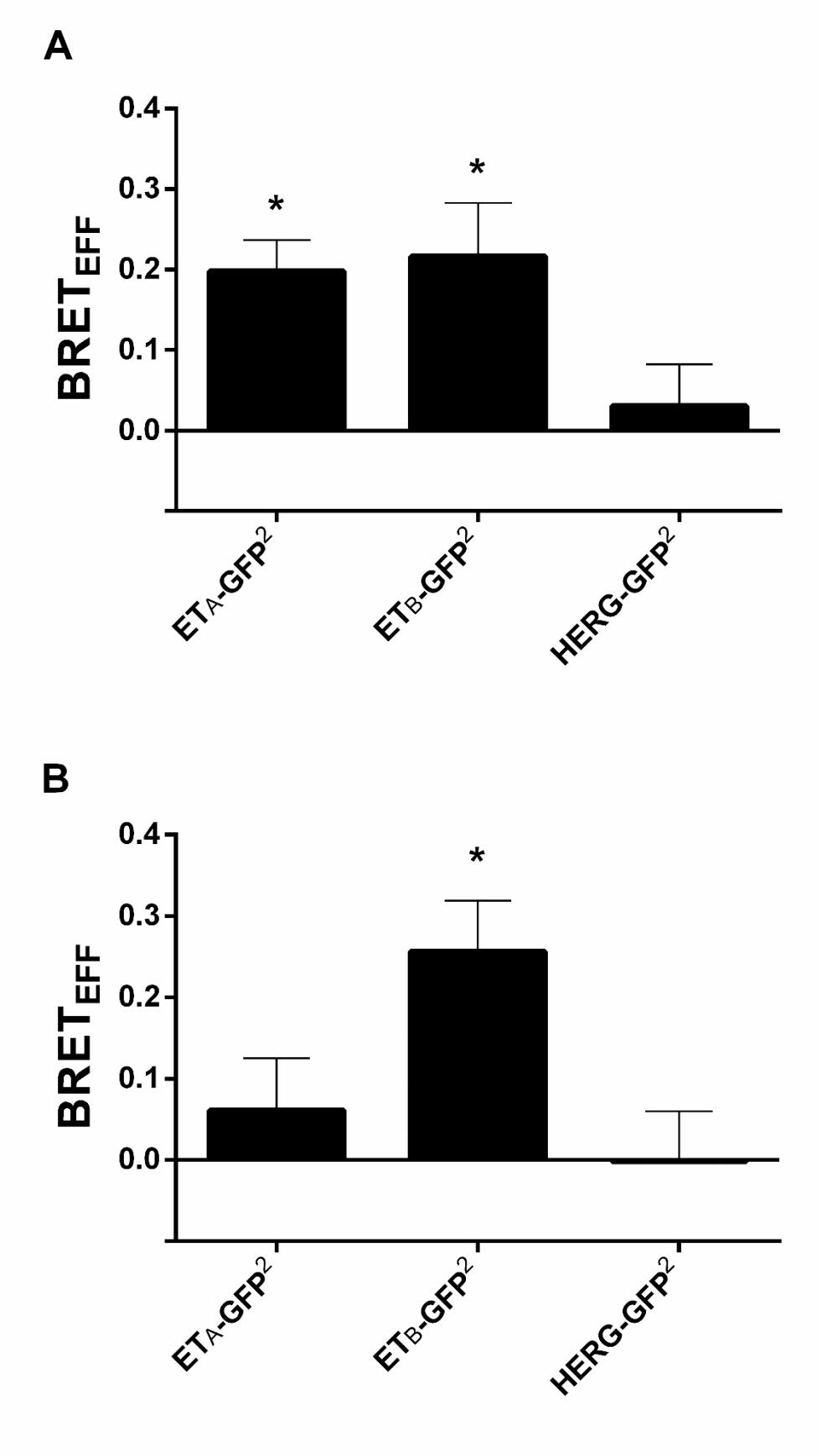
A
0.4
0.3
0.2
0.1
0.0
BRET EFF
*
*
ETA-GFP2
ETB-GFP2
HERG-GFP2
B
0.4
0.3
0.2
0.1
0.0
BRET EFF
*
ETA-GFP2
ETB-GFP2
HERG-GFP2

Table 3.1: Endothelin receptor BRET saturation curve data

Interaction	$BRET_{MAX}$	$BRET_{50}$	Hyperbolic Fit (R^2)	Linear Fit (R^2)
ET_A-Rluc + ET_A-GFP²	0.358 ± 0.070	2.624 ± 0.875	0.834	0.962
ET_B-Rluc + ET_B-GFP²	0.280 ± 0.002	0.430 ± 0.013	0.982	0.537
ET_A-Rluc + ET_B-GFP²	0.290 ± 0.002	0.482 ± 0.013	0.986	0.568
ET_A-Rluc + HERG-GFP²	0.043 ± 0.004	ND	0	0.003
ET_B-Rluc + HERG-GFP²	0.034 ± 0.000	ND	0.521	0.053

ND: Not determined

Figure 3.2: *Evidence for ET_A receptor homodimerization was inconclusive*

BRET saturation curves obtained from HEK293 cells transiently transfected with 1 µg ET_A-Rluc and increasing ET_A-GFP^2 (solid line, circles; n=4) or HERG-GFP^2 (dashed line, triangles; n=3). $BRET_{EFF}$ is plotted against the mass ratio of GFP^2 and Rluc tagged constructs used during transfection.

Data were fit to equation #2 (page 28), with additional linear regression in dotted red.

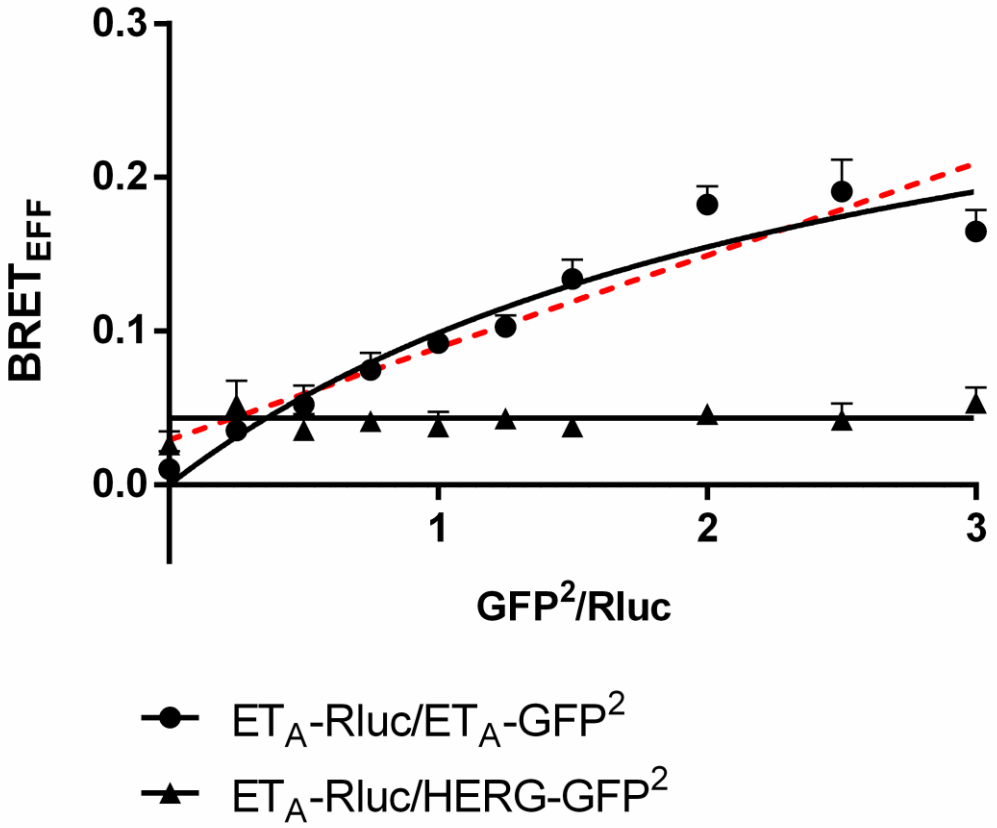
0.3
0.2
0.1
0.0
BRET$_{EFF}$
1
2
3
GFP^2/Rluc
ET$_A$-Rluc/ET$_A$-GFP^2
ET$_A$-Rluc/HERG-GFP^2

Figure 3.3: *ET_B receptors formed homodimers*

BRET saturation curves obtained from HEK293 cells transiently transfected with 1 µg ET_B-Rluc and increasing ET_B-GFP^2 (solid line, circles; n=4) or HERG-GFP^2 (dashed line, triangles; n=3). $BRET_{EFF}$ is plotted against the mass ratio of GFP^2 and Rluc tagged constructs used during transfection. Data were fit to equation #2 (page 28).

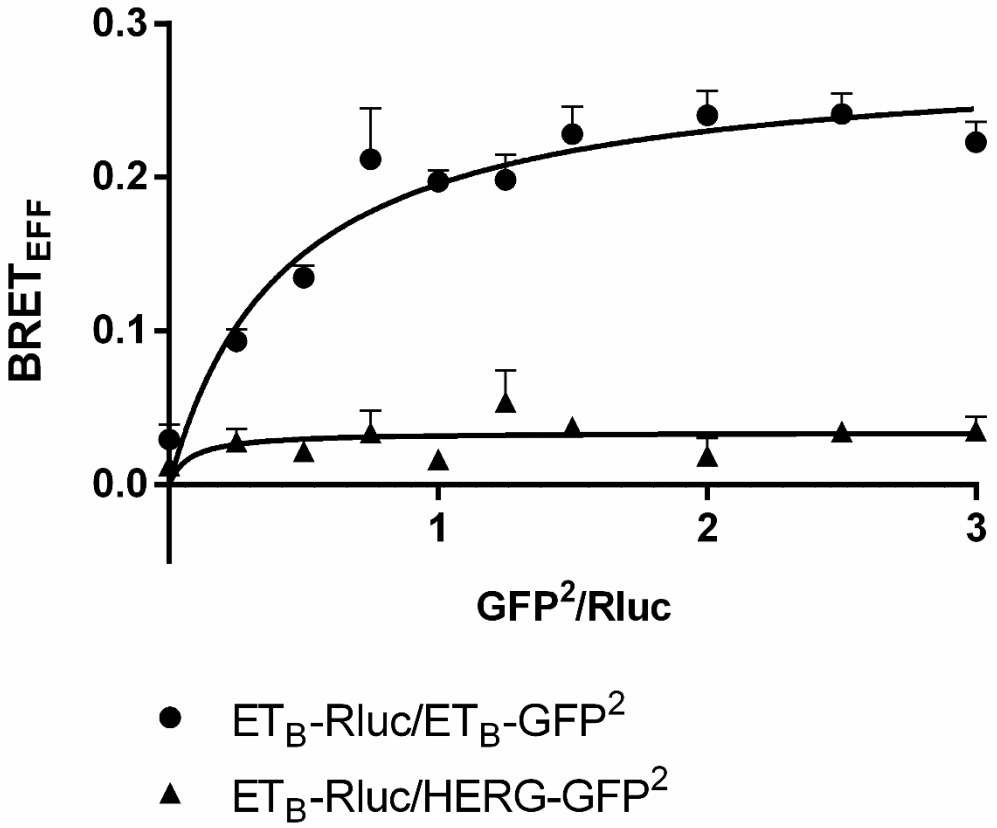
0.3
0.2
0.1
0.0
BRET$_{EFF}$
1
2
3
GFP^2/Rluc
ET$_B$-Rluc/ET$_B$-GFP^2
ET$_B$-Rluc/HERG-GFP^2

Figure 3.4: *ET_A and ET_B receptors formed heterodimers*

BRET saturation curves obtained from HEK293 cells transiently transfected with 1 µg ET_A-Rluc and increasing ET_B-GFP^2 (solid line, circles; n=4) or HERG-GFP^2 (dashed line, triangles; n=3). $BRET_{EFF}$ is plotted against the mass ratio of GFP^2 and Rluc tagged constructs used during transfection. Data were fit to equation #2 (page 28).

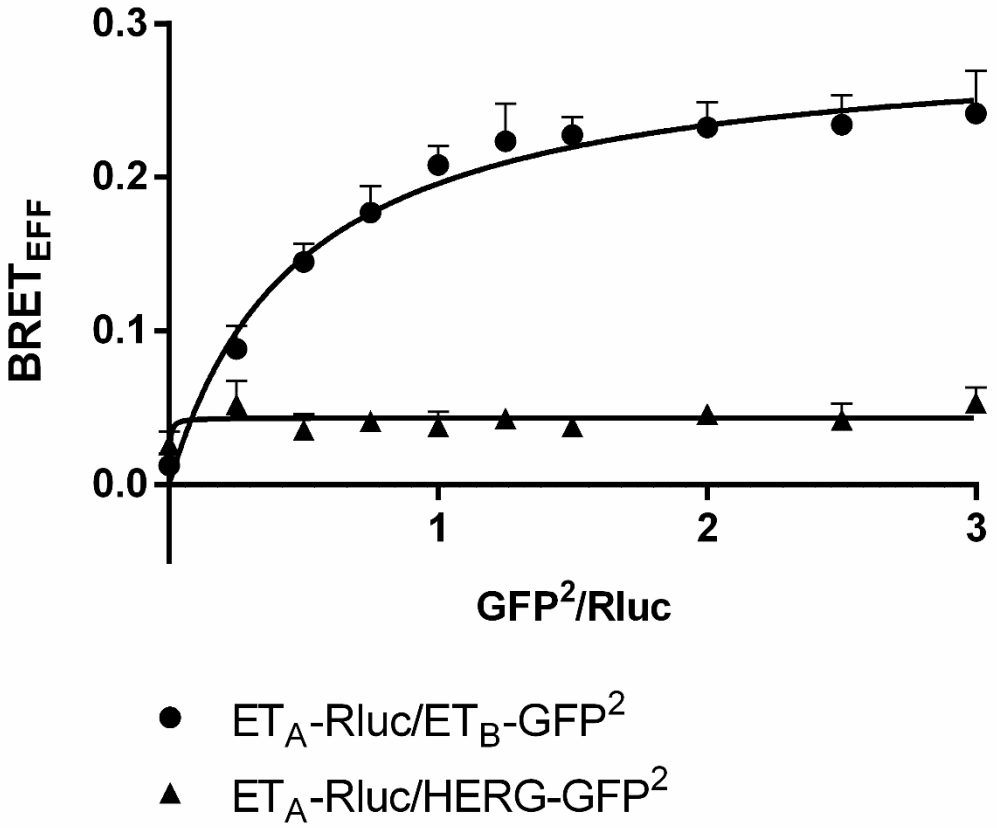
0.3
0.2
0.1
0.0
BRET$_{EFF}$
1
2
3
GFP^2/Rluc
ET$_A$-Rluc/ET$_B$-GFP^2
ET$_A$-Rluc/HERG-GFP^2

ET_A/ET_A interactions were found to be of relatively lower affinity ($BRET_{50}$ = 2.624 ± 0.875) compared to ET_B homodimers ($BRET_{50}$ = 0.430 ± 0.013) and ET_A/ET_B heterodimers ($BRET_{50}$ = 0.482 ± 0.013).

3.2 β-arrestin-1 Recruitment to Endothelin Receptors

The next objective was to test if endothelin receptor heterodimerization inhibited the function of β-arrestin, beginning first with its recruitment. For this, I sought to determine if ET-1 induced β-arrestin-1 recruitment in HEK293 cells using $BRET^2$ methodology. HEK293 cells were transfected with 1 µg ET_A-Rluc and 0 to 3 µg β-arrestin-1-GFP^2 (n=4) (Fig. 3.5A) as well as with 1 µg ET_B-Rluc and 0 to 3 µg β-arrestin-1-GFP^2 (n=4) (Fig. 3.5B). BRET measurements were performed 20 minutes after treatment with either vehicle (DMEM) or 10 nM ET-1. Corresponding BRET data are summarized in Table 3.2.

In the case of both ET_A and ET_B, $BRET_{MAX}$ values were not significantly different between vehicle and ET-1 treatment, indicating that interactions between endothelin receptors and β-arrestin-1 were not enhanced by receptor activation. Therefore, β-arrestin-1 potentially only forms constitutive interactions with endothelin receptors.

Table 3.2: Endothelin receptor β-arrestin-1-GFP^2 recruitment BRET saturation data

Interaction	$BRET_{MAX}$	$BRET_{50}$	Hyperbolic Fit (R^2)	Linear Fit (R^2)
ET_A-Rluc + Vehicle	0.070 ± 0.014	0.695 ± 0.434	0.633	0.833
ET_A-Rluc + ET-1	0.078 ± 0.012	0.553 ± 0.306	0.687	0.798
ET_B-Rluc + Vehicle	0.048 ± 0.010	0.553 ± 0.010	0.506	0.798
ET_B-Rluc + ET-1	0.071 ± 0.016	1.067 ± 0.604	0.613	0.889

Figure 3.5: *ET_A and ET_B receptors constitutively interacted with β-arrestin-1*

A. BRET saturation curves obtained from HEK293 cells transiently transfected with 1 µg ET_A-Rluc and increasing β-arrestin-1-GFP^2 treated with either vehicle (dashed line, circles) or 10 nM ET-1 (solid lines, triangles). **B.** BRET saturation curves obtained from HEK293 cells transiently transfected with 1 µg ET_B-Rluc and increasing β-arrestin-1-GFP^2 treated with either vehicle (dashed line, circles) or 10 nM ET-1 (solid lines, triangles). $BRET_{EFF}$ is plotted against the mass ratio of GFP^2 and Rluc tagged constructs used during transfection. Data were fit to equation #2 (page 28); n=4.

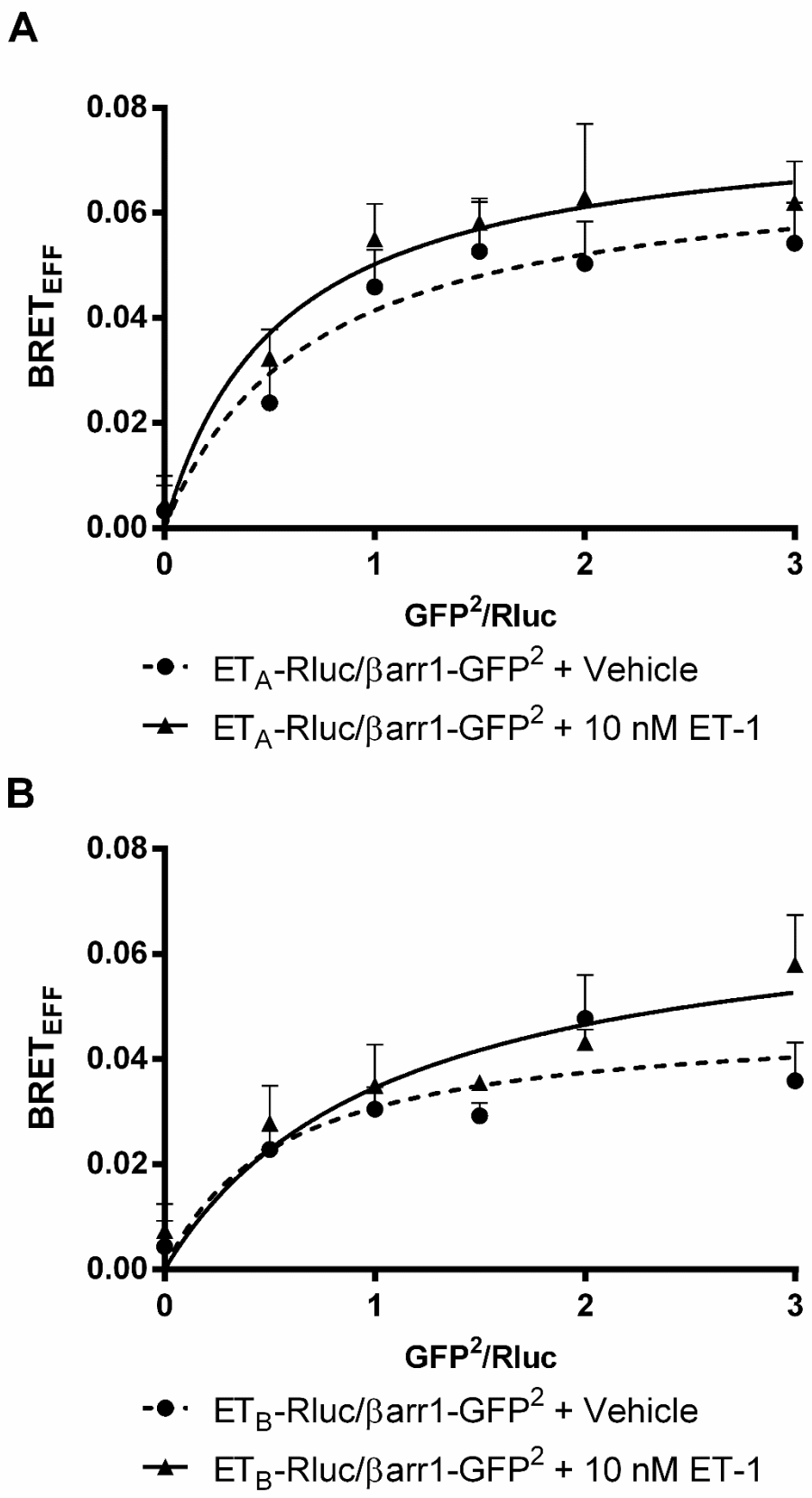
A
0.08
0.06
0.04
0.02
0.00
BRET$_{EFF}$
0
1
2
3
GFP^2/Rluc
ET$_A$-Rluc/βarr1-GFP^2 + Vehicle
ET$_A$-Rluc/βarr1-GFP^2 + 10 nM ET-1
B
0.08
0.06
0.04
0.02
0.00
BRET$_{EFF}$
0
1
2
3
GFP^2/Rluc
ET$_B$-Rluc/βarr1-GFP^2 + Vehicle
ET$_B$-Rluc/βarr1-GFP^2 + 10 nM ET-1

3.3 β-arrestin-2 Recruitment to Endothelin Receptors

I then used BRET technology to test if β-arrestin-2 is recruited to endothelin receptors. HEK293 cells were transfected with 0.5 µg ET_A-Rluc and 0 to 1.5 µg β-arrestin-2-GFP^2 ± 0.5 µg untagged ET_B and BRET measurements were performed 20 minutes after vehicle or 10 nM ET-1 treatment (Fig. 3.6), with corresponding BRET data summarized in Table 3.3.

In both the presence and absence of ET_B, $BRET_{MAX}$ values were significantly higher in the 10 nM ET-1 treated cells compared to vehicle, indicating that ET-1 agonism initiated additional β-arrestin-2-GFP^2 recruitment. Compared to cells transfected only with ET_A-Rluc, co-transfection with untagged ET_B significantly decreased $BRET_{MAX}$ in ET-1 treated cells, indicative of a reduced maximal β-arrestin-2 recruitment.

Table 3.3: *ET_A-Rluc recruitment of β-arrestin-2-GFP^2 BRET saturation curve data in the presence or absence of ET_B*

Interaction	$BRET_{MAX}$	$BRET_{50}$	Hyperbolic Fit (R^2)	Linear Fit (R^2)
ET_A-Rluc + Vehicle	0.110 ± 0.035	0.453 ± 0.573	0.580	0.621
ET_A-Rluc + ET-1	0.326 ± 0.051	0.702 ± 0.340	0.894	0.533
ET_A-Rluc + ET_B + Vehicle	0.085 ± 0.031	0.515 ± 0.686	0.763	0.812
ET_A-Rluc + ET_B + ET-1	0.210 ± 0.027	0.555 ± 0.253	0.945	0.654

Figure 3.6: *Co-expression of ET_B inhibited ET_A recruitment of β-arrestin-2*

BRET saturation curves obtained from HEK293 cells transiently transfected with 0.5 µg ET_A-Rluc and increasing β-arrestin-2-GFP^2 treated with: vehicle (dashed line, black circles) or 10 nM ET-1 (solid line, black circles); or 0.5 µg ET_A-Rluc, 0.5 µg ET_B, and increasing β-arrestin-2-GFP^2 treated with: vehicle (dashed line, white squares) or 10 nM ET-1 (solid line, white squares). $BRET_{EFF}$ is plotted against the mass ratio of GFP^2 and Rluc tagged constructs used during transfection. Data were fit to equation #2 (page 28); * $P<0.05$ between calculated $BRET_{MAX}$ values; n=3.

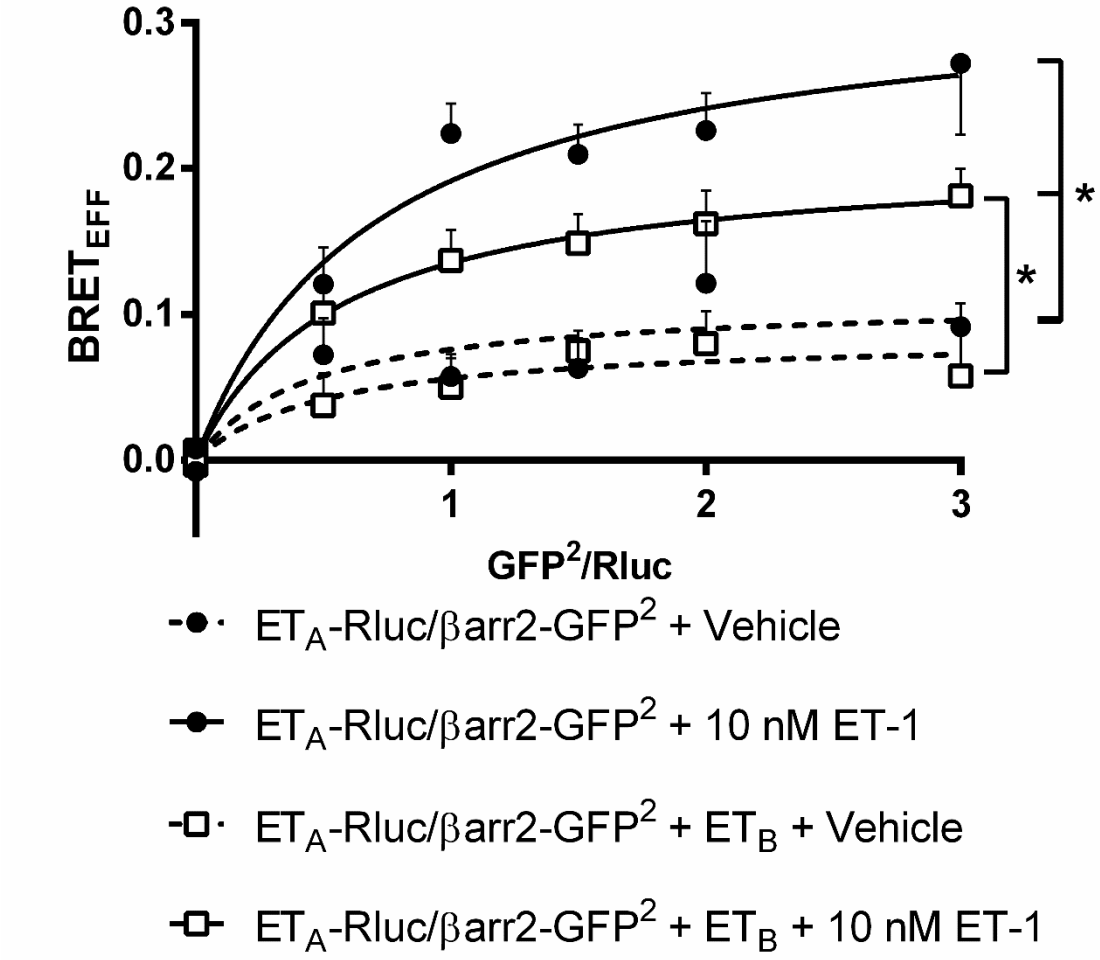
0.3
0.2
0.1
0.0
BRET$_{EFF}$
1
2
3
GFP^2/Rluc
*
*
ET$_A$-Rluc/βarr2-GFP^2 + Vehicle
ET$_A$-Rluc/βarr2-GFP^2 + 10 nM ET-1
ET$_A$-Rluc/βarr2-GFP^2 + ET$_B$ + Vehicle
ET$_A$-Rluc/βarr2-GFP^2 + ET$_B$ + 10 nM ET-1

Similar experiments were also conducted examining β-arrestin-2 recruitment to ET_B-Rluc. HEK293 cells were transfected with 0.5 µg ET_B-Rluc and 0 to 1.5 µg β-arrestin-2-GFP^2 ± 0.5 µg untagged ET_A and BRET measurements were performed 20 minutes after either vehicle or 10 nM ET-1 treatment (Fig. 3.7), with corresponding BRET data summarized in Table 3.4.

In this case, $BRET_{MAX}$ was significantly increased after ET-1 exposure in ET_B-Rluc transfected cells but not in cells co-transfected with both receptor subtypes. Interestingly, co-transfection of untagged ET_A alongside ET_B-Rluc significantly reduced $BRET_{MAX}$ compared to transfections lacking untagged ET_A in ET-1 treated cells; this would be consistent with a heterodimer-mediated inhibition of β-arrestin-2 recruitment. Alternatively, there is also the possibility that the untagged monomeric or homodimeric ET_B was being activated by ET-1 and recruiting β-arrestin-2-GFP^2 from a limited pool. This would effectively decrease $BRET_{EFF}$ by limiting the amount of β-arrestin-2 available for recruitment to ET_A; although based on the saturation curve data we can begin to observe a decrease in $BRET_{EFF}$ at as low as a 1:1 ratio of β-arrestin-2-GFP^2 to ET_A-Rluc when co-transfecting ET_B. This makes it unlikely that ET_B is simply sequestering β-arrestin-2-GFP^2 at the 3:1 ratio point.

Table 3.4: *ET_B-Rluc recruitment of β-arrestin-2-GFP^2 BRET saturation curve data in the presence or absence of ET_A*

Interaction	$BRET_{MAX}$	$BRET_{50}$	Hyperbolic Fit (R^2)	Linear Fit (R^2)
ET_B-Rluc + Vehicle	0.213 ± 0.046	0.910 ± 0.531	0.836	0.695
ET_B-Rluc + ET-1	0.367 ± 0.040	0.657 ± 0.229	0.938	0.571
ET_B-Rluc + ET_A + Vehicle	0.204 ± 0.066	1.470 ± 1.047	0.902	0.743
ET_B-Rluc + ET_A + ET-1	0.235 ± 0.033	0.547 ± 0.276	0.984	0.612

Figure 3.7: *Co-expression of ET_A inhibited ET_B recruitment of β-arrestin-2*

BRET saturation curves obtained from HEK293 cells transiently transfected with 0.5 µg ET_B-Rluc and increasing β-arrestin-2-GFP^2 treated with: vehicle (dashed line, black circles) or 10 nM ET-1 (solid line, black circles); or 0.5 µg ET_B-Rluc, 0.5 µg ET_A, and increasing β-arrestin-2-GFP^2 treated with: vehicle (dashed line, white squares) or 10 nM ET-1 (solid line, white squares). $BRET_{EFF}$ is plotted against the mass ratio of GFP^2 and Rluc tagged constructs used during transfection. Data were fit to equation #2 (page 28); * $P<0.05$ between calculated $BRET_{MAX}$ values; n=3.

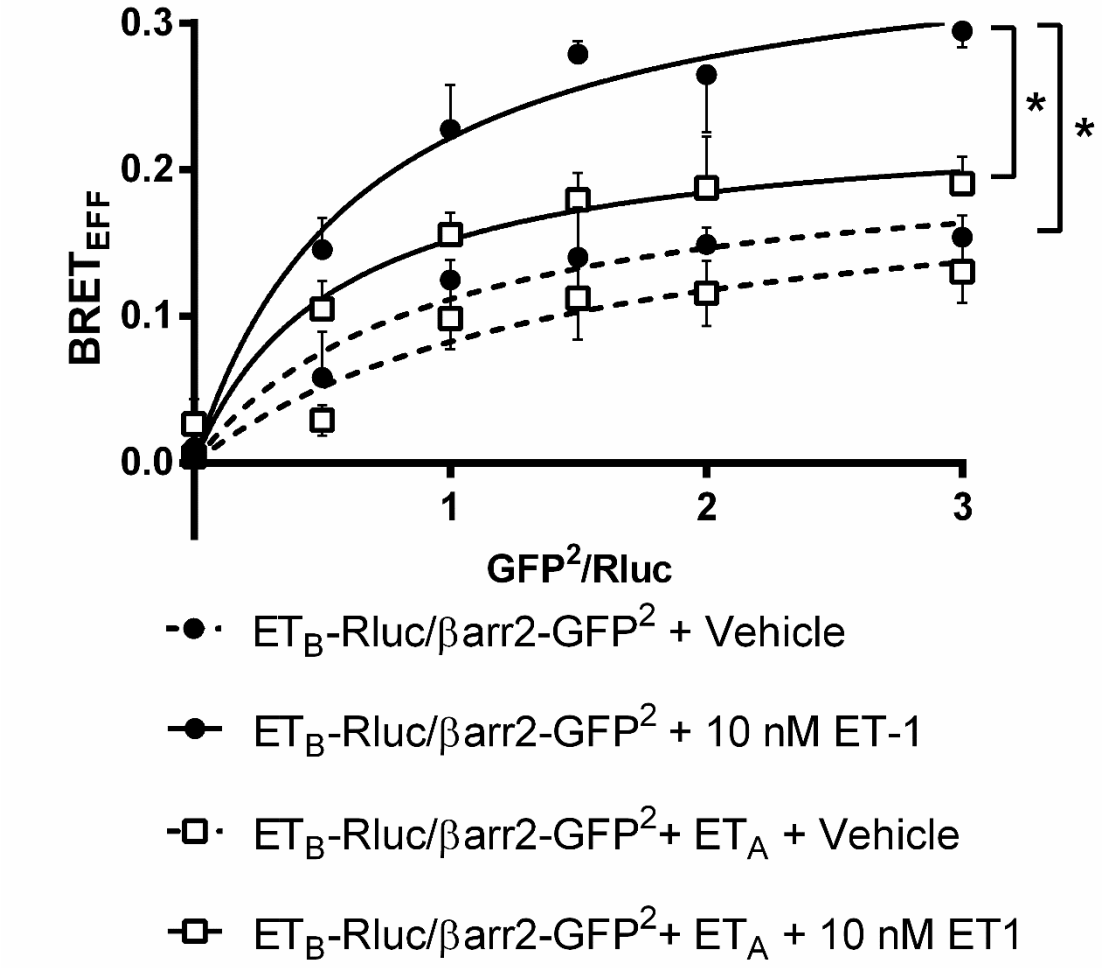
0.3
0.2
0.1
0.0
BRET_EFF
1
2
3
GFP²/Rluc
*
*
ET_B-Rluc/βarr2-GFP² + Vehicle
ET_B-Rluc/βarr2-GFP² + 10 nM ET-1
ET_B-Rluc/βarr2-GFP²+ ET_A + Vehicle
ET_B-Rluc/βarr2-GFP²+ ET_A + 10 nM ET1

I next wanted to test if co-expression of both endothelin receptor subtypes delayed β-arrestin-2 recruitment. To do this, HEK293 cells were treated with 10 nM ET-1 48 hours after transfection with either 0.5 µg ET_A-Rluc and 1.5 µg β-arrestin-2-GFP^2 (1.5 µg) ± 0.5 µg untagged ET_B (Fig. 3.8A), or the reciprocal 0.5 µg ET_B-Rluc and 1.5 µg β-arrestin-2-GFP^2 ± 0.5 µg untagged ET_A (Fig. 3.8B). Co-transfection of untagged ET_B with ET_A-Rluc significantly decreased $BRET_{EFF}$ at 5-15 and 30 minutes, while co-transfection of untagged ET_A with ET_B-Rluc significantly decreased $BRET_{EFF}$ from 5-30 minutes, suggesting an inhibition of β-arrestin-2-GFP^2 recruitment. The time to half-maximal recruitment was significantly longer in cells transfected with ET_A-Rluc and ET_B (10.6 ± 2.8 minutes), compared to cells transfected with ET_A-Rluc (3.1 ± 5.2 minutes). In the reciprocal experiments, time to half-maximal recruitment was significantly longer in cells co-transfected with ET_B-Rluc and ET_A (9.4 ± 1.5 minutes) compared to cells transfected with only ET_B-Rluc (3.2 ± 1.2 minutes). Together, these experiments provided evidence that co-expression of both endothelin receptor subtypes decreased and delayed β-arrestin-2 recruitment. It cannot be accurately stated that this was necessarily an effect of heterodimerization, as the inclusion of the reciprocal receptor subtype could have been creating competition for a limited pool of β-arrestin-2. The latter was partially addressed in the experimental design by expressing β-arrestin-2 at an increased ratio to the endothelin receptors. Furthermore, previous $BRET^2$ saturation curves showed ET_A/ET_B heterodimer formation was already maximal at a 1:1 ET_A:ET_B ratio, so untagged receptor was co-transfected at this level in β-arrestin-2 recruitment assays.

Figure 3.8: *Co-expression of ET_A and ET_B delayed ET-1-induced β-arrestin-2 recruitment*

A. Time-course of β-arrestin-2 recruitment to endothelin receptors following 10 nM ET-1 treatment in HEK293 cells transiently transfected with 0.5 µg ET_A-Rluc and 1.5 µg β-arrestin-2-GFP^2 (black) and 0.5 µg ET_B (white). **B.** Time-course of β-arrestin-2 recruitment to endothelin receptors following 10 nM ET-1 treatment in HEK293 cells transiently transfected with 0.5 µg ET_B-Rluc and 1.5 µg β-arrestin-2-GFP^2 (black) and 0.5 µg ET_A (white). $BRET_{EFF}$ is plotted against time in minutes following ET-1 treatment. Data were fit to equation #3 (page 28); * $P<0.05$; n=3.

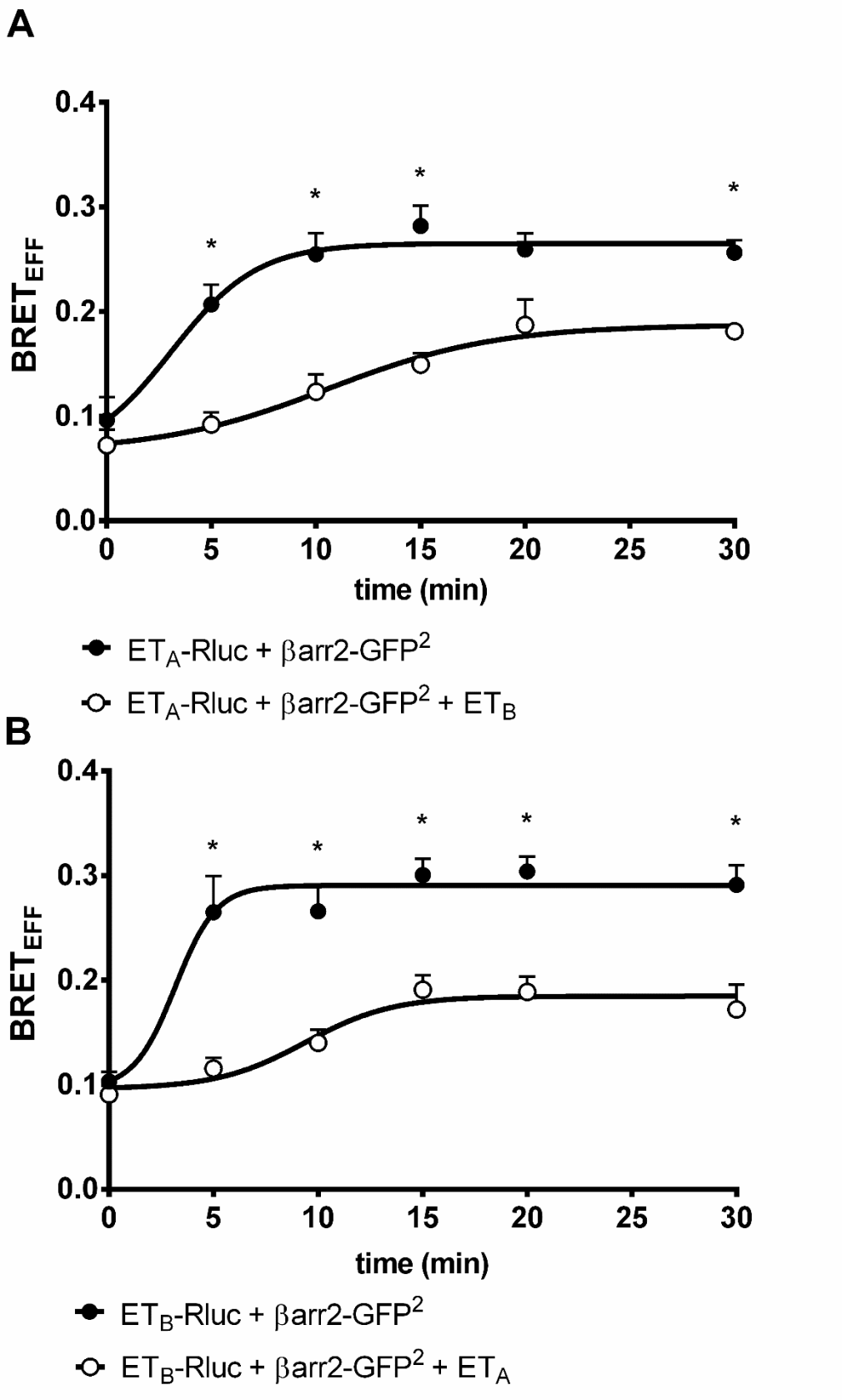
A
0.4
0.3
0.2
0.1
0.0
BRET_EFF
0
5
10
15
20
25
30
time (min)
ET_A-Rluc + βarr2-GFP^2
ET_A-Rluc + βarr2-GFP^2 + ET_B
B
0.4
0.3
0.2
0.1
0.0
BRET_EFF
0
5
10
15
20
25
30
time (min)
ET_B-Rluc + βarr2-GFP^2
ET_B-Rluc + βarr2-GFP^2 + ET_A

To further demonstrate that the delayed β-arrestin-2 recruitment was heterodimer-specific, the previous experiment was repeated using ET_B-selective agonist, BQ-3020. Because BQ-3020 does not appreciably bind or activate ET_A at the concentration used (Ihara *et al*., 1992), this approach ensured that ET_A acted only as a physically interacting protein to ET_B. HEK293 cells were treated with 10 nM BQ-3020 48 hours after transfection with either 0.5 µg ET_A-Rluc and 1.5 µg β-arrestin-2-GFP^2 (1.5 µg) ± 0.5 µg untagged ET_B (Fig. 3.9A), or the reciprocal 0.5 µg ET_B-Rluc and 1.5 µg β-arrestin-2-GFP^2 ± 0.5 µg untagged ET_A (Fig. 3.9B). ET_B-selective agonism did not significantly increase $BRET_{EFF}$ in cells transfected with ET_A-Rluc ± ET_B, suggesting that ET_A is not recruiting β-arrestin-2-GFP^2.

In contrast, in HEK293 cells transfected with ET_B-Rluc ± ET_A, selective ET_B agonism with BQ-3020 caused a rapid increase in $BRET_{EFF}$, which was significantly lower at 5 and 10 minutes in cells co-transfected with untagged ET_A. Time to half-maximal recruitment was significantly longer in cells co-transfected with ET_B-Rluc and ET_A (9.7 ± 2.0 minutes) compared to cells transfected with only ET_B-Rluc (4.6 ± 2.1 minutes). As ET_A appeared incapable of recruiting β-arrestin-2 with BQ-3020 treatment, the co-transfected ET_A likely mediated its effect through physical interaction with ET_B. These experiments showed that BQ-3020 selectively activated ET_B and that the ET_A/ET_B heterodimer was likely delaying β-arrestin-2 recruitment.

Figure 3.9: *Co-expression of ET_A and ET_B delayed β-arrestin-2 recruitment following ET_B-specific agonism*

A. Time-course of β-arrestin-2 recruitment to endothelin receptors following 10 nM BQ-3020 treatment in HEK293 cells transiently transfected with 0.5 µg ET_A-Rluc and 1.5 µg β-arrestin-2-GFP^2 (black) and 0.5 µg ET_B (white). **B.** Time-course of β-arrestin-2 recruitment to endothelin receptors following 10 nM BQ-3020 treatment in HEK293 cells transiently transfected with 0.5 µg ET_B-Rluc and 1.5 µg β-arrestin-2-GFP^2 (black) and 0.5 µg ET_A (white). $BRET_{EFF}$ is plotted against time in minutes after agonist treatment. Data were fit to equation #3 (page 28); * $P<0.05$; n=3.

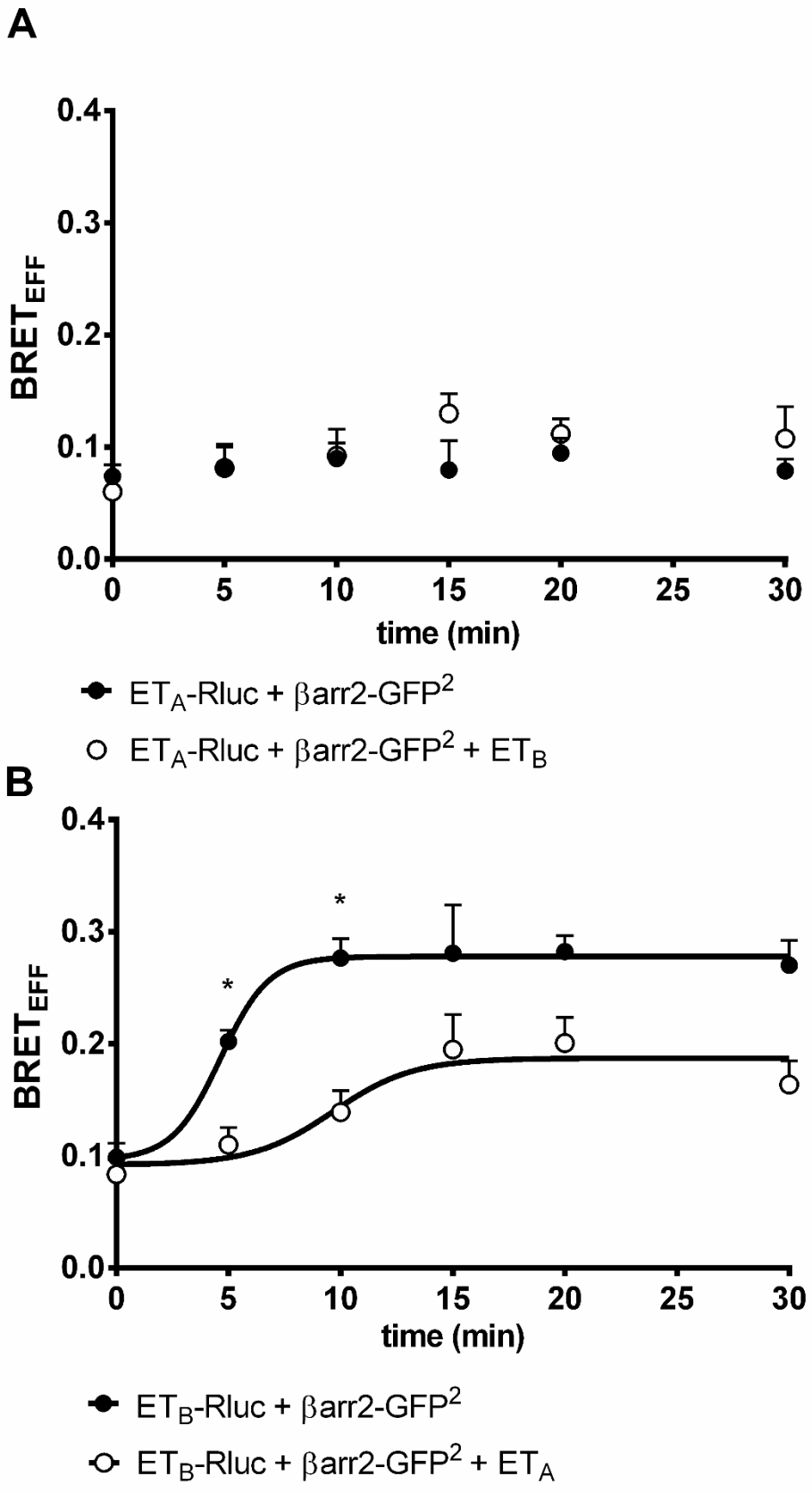
A
0.4
0.3
0.2
0.1
0.0
BRET_EFF
0
5
10
15
20
25
30
time (min)
ET_A-Rluc + βarr2-GFP^2
ET_A-Rluc + βarr2-GFP^2 + ET_B
B
0.4
0.3
0.2
0.1
0.0
BRET_EFF
*
*
0
5
10
15
20
25
30
time (min)
ET_B-Rluc + βarr2-GFP^2
ET_B-Rluc + βarr2-GFP^2 + ET_A

3.4 ERK Phosphorylation Downstream of Endothelin Receptor Activation

To test if this heterodimer-mediated inhibition of β-arrestin recruitment can potentially alter cell function, In-cell Western® was used to assay for ERK phosphorylation, a signaling molecule directly activated by the GPCR-β-arrestin complex as well as by G-protein-dependent kinase cascades. HEK293 cells transfected with 0.5 µg untagged ET_A ± 0.5 µg untagged ET_B ± 1 µg β-arrestin-1 dominant negative (Val-53ΔAsp) (β-arr -) were treated with 10 nM ET-1 and fixed 5 or 20 minutes later. *Pertussis* toxin (PTX) was applied 24 hours prior to ET-1 treatment, and 100 nM PKC inhibitor Gö-6983 one-hour prior to ET-1 treatment. In-cell Western® was then used to assay for ERK and p-ERK (Fig. 3.10). PTX pre-treatment did not alter ERK phosphorylation 5 or 20 minutes after ET-1 treatment, indicating that endothelin receptors may not couple with Gαi and that ET-1-mediated ERK phosphorylation is Gαi-independent.

Compared to ET-1 treatment, co-transfection with dominant negative β-arrestin-1 significantly decreased ERK phosphorylation at 5 and 20 minutes in ET_A-transfected cells, but not in cells co-transfected with both ET_A and ET_B. This suggests that β-arrestin was mediating a proportion of ERK phosphorylation downstream of endothelin receptor activation. To examine if G-protein signalling is also altered by endothelin receptor co-expression, PKC inhibitor Gö-6983 was used to inhibit ERK phosphorylation by PKC, a kinase protein activated downstream of Gαq activation. PKC inhibition significantly decreased ERK phosphorylation at 5 minutes following ET-1 treatment in ET_A-transfected HEK293.

Figure 3.10: *ET_A mediated ERK phosphorylation was Gαq- and β-arrestin-1-dependent*

HEK293 cells transfected with 0.5 µg ET_A (black bars) or 0.5 µg ET_A and 0.5 µg ET_B (white bars) were fixed (**A**) 5 or (**B**) 20 minutes after treatment with 10 nM ET-1 for processing with In-cell Western® against ERK and pERK. Treatments include 24-hour pre-incubation with pertussis toxin (PTX), co-transfection with β-arrestin-1 dominant negative (β-arr -), and one-hour pre-incubation with 100 nM PKC inhibitor Gö-6983. Data presented as percent change relative to vehicle treatment; * $P<0.05$ relative to ET-1 treatment; n=3-5.

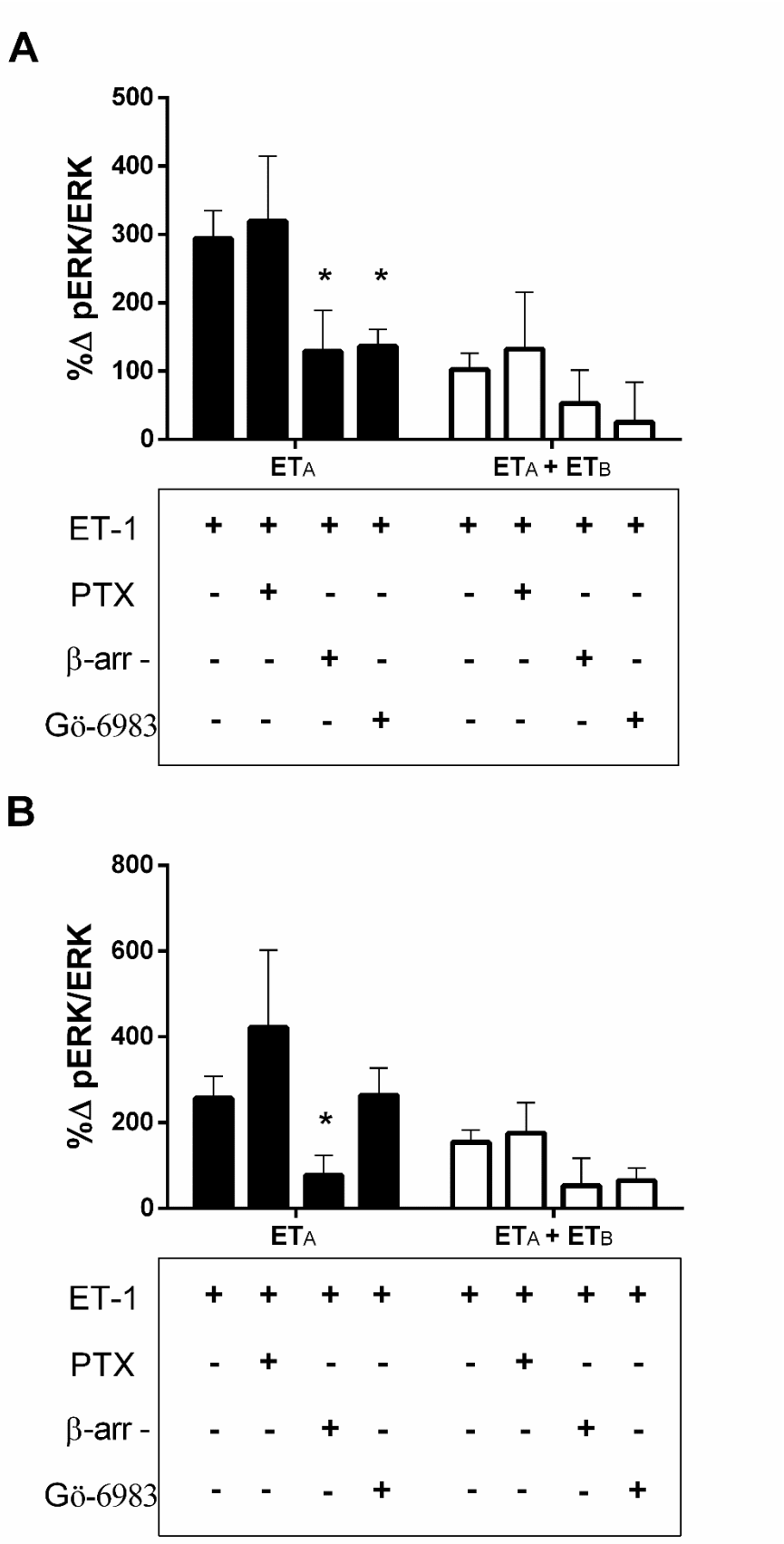
A
500
400
300
200
100
0
%Δ pERK/ERK
*
*
ETA
ETA + ETB
ET-1 + + + + + + + +
PTX - + - - - + - -
β-arr - - - + - - - + - -
Gö-6983 - - - + - - - +
B
800
600
400
200
0
%Δ pERK/ERK
*
ETA
ETA + ETB
ET-1 + + + + + + + +
PTX - + - - - + - -
β-arr - - - + - - - + - -
Gö-6983 - - - + - - - +

Next, the time-course for ERK phosphorylation was examined in HEK293 cells transfected with 0.5 µg untagged ET_A ± 0.5 µg untagged ET_B. Cells were treated with 10 nM ET-1 and then fixed at selected time points, followed by In-cell Western® to assay for ERK phosphorylation (Fig. 3.11). ERK phosphorylation was significantly lower at 3 and 5 minutes in HEK293 cells co-transfected with ET_A and ET_B compared to HEK293 cells transfected with only ET_A.

Figure 3.11: *ET-1 mediated ERK phosphorylation was delayed by co-expression of both ET_A and ET_B*

HEK293 cells transfected with 0.5 µg ET_A (black circles) or 0.5 µg ET_A and 0.5 µg ET_B (white circles) were treated with 10 nM ET-1 and fixed at selected time points for processing with In-cell Western® against ERK and pERK. Data presented as percent change relative to t=0 min; n=5.

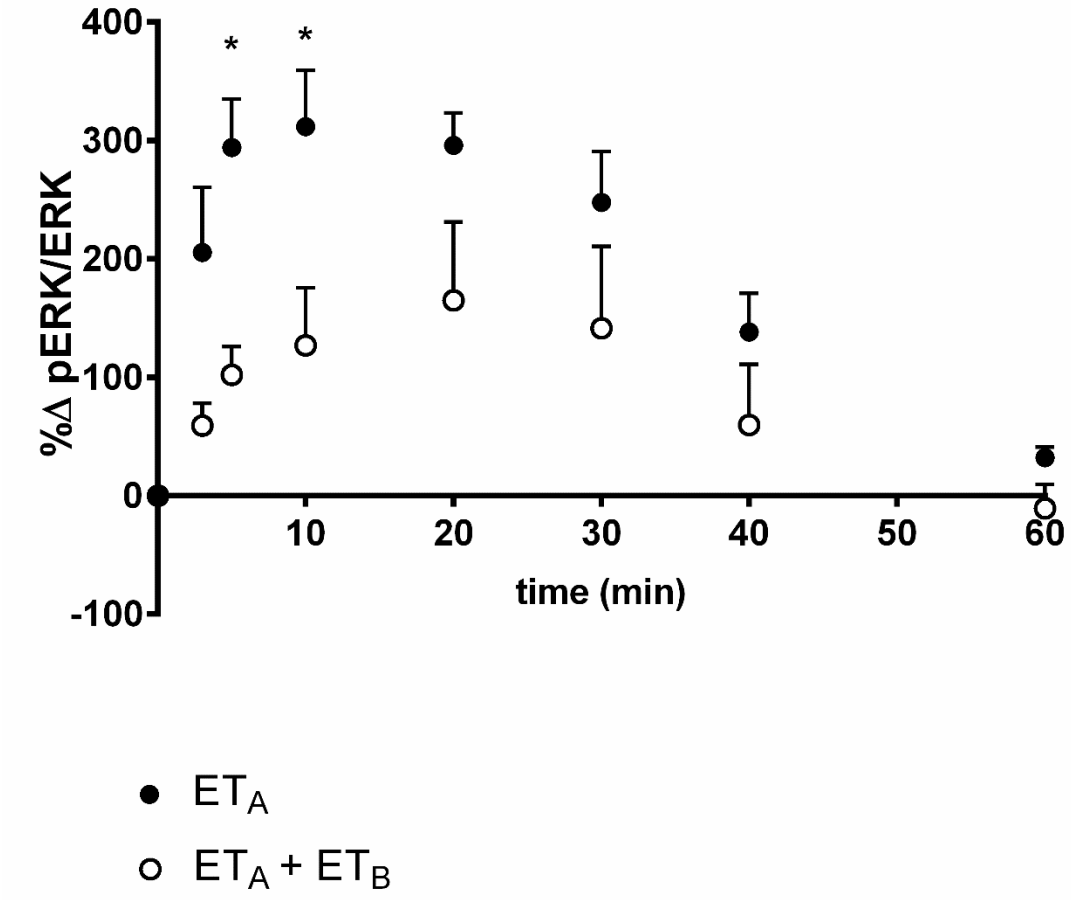
400
300
200
100
0
-100
%Δ pERK/ERK
*
*
10
20
30
40
50
60
time (min)
ET$_A$
ET$_A$ + ET$_B$

Chapter 4: Discussion

GPCRs can function as monomeric units (Whorton *et al.*, 2007), but an increasing body of knowledge supports GPCR dimerization or oligomerization as the native physiological state (Bouvier and Hebert, 2014). GPCR dimerization has been documented to profoundly impact receptor dynamics (Gurevich and Gurevich, 2008). Endothelin receptor heterodimerization is an important topic of study because it prolongs calcium transients, and likely plays an important role in endothelin physiology in tissues co-expressing both receptor subtypes. The main focus of my thesis was to test the hypothesis that endothelin receptor heterodimerization inhibits β-arrestin function.

My objectives were to quantify the affinity of endothelin receptor physical interactions, and explore how these might impact β-arrestin recruitment and the β-arrestin-dependent ERK signaling cascade. Using $BRET^2$ as a means to observe physical interactions via energy transfer, I demonstrated that ET_A and ET_B formed heterodimers, and ET_B formed homodimers, while evidence supporting ET_A homodimerization was inconclusive. β-arrestin-2, but not β-arrestin-1, was recruited to ET_A or ET_B following application of the non-selective endothelin receptor agonist ET-1 in $BRET^2$ assays. Co-expression of both ET_A and ET_B reduced and delayed β-arrestin-2 recruitment. ERK phosphorylation following the application of ET-1 was not altered by PTX treatment, suggesting it was Gαi-independent. ET-1-induced ERK phosphorylation was both β-arrestin-1- and PKC-dependent in HEK293 expressing ET_A, while cells co-expressing ET_A and ET_B were not significantly affected by Gαi, β-arrestin-1, or PKC inhibition.

***4.1** ET_A and ET_B receptors heterodimerize and ET_B receptors homodimerize*

In the present study, endothelin receptor dimer combinations were compared in their specificity and affinity. A previous study examining endothelin receptor dimerization with FRET reported that ET_A and ET_B both homo- and heterodimerize (Evans and Walker, 2008). FRET is a qualitative method that simply allows for the visualization of protein-protein interactions *in situ*, and observing dimerization with FRET can potentially be an artifact arising from overexpression of the fusion proteins (Day *et al.*, 2001). $BRET^2$ overcomes this limitation by allowing for quantitative measurement of the specificity of an interaction (Pfleger and Eidne, 2003). $BRET^2$ saturation curves for ET_A-Rluc and ET_A-GFP^2 did not conclusively demonstrate ET_A homodimerization, as both linear (R^2 = 0.962) and hyperbolic (R^2 = 0.834) regression provided adequate fits. This experiment should be further extended by testing higher ratios of ET_A-GFP^2 to ET_A-Rluc to examine if the interaction is truly saturable. Regardless, the putative affinity of the interaction given by non-linear regression ($BRET_{50}$ = 2.624 ± 0.875) indicates that even if ET_A homodimerization does occur, it is not likely a dominant species within a mixed population of endothelin receptors.

ET_B homodimers and ET_A/ET_B heterodimers displayed specific and saturable associations with similar affinity to form interactions ($BRET_{50}$ = 0.430 ± 0.013 and 0.482 ± 0.013, respectively). It is worth noting that $BRET_{EFF}$ values reflect a mixed receptor population; when co-expressing ET_A-Rluc and ET_B-GFP^2, the only observable contribution to $BRET_{EFF}$ are ET_A-Rluc/ET_B-GFP^2 heterodimers, but ET_A-Rluc and ET_B-GFP^2 homodimers and monomers could also be present.

This being said, BRET measurement does not give any indication towards the existence of higher-order geometries, and therefore the term “dimers”, as measured with BRET in this study, represents the minimal oligomeric state, and may actually be components of unseen oligomers (Gandia *et al.*, 2008).

***4.2** β-arrestin-2, but not β-arrestin-1, was recruited to endothelin receptors*

Endothelin receptors have previously been classified as “Class A” GPCRs that bind β-arrestin-2 with a higher affinity than β-arrestin-1 (Oakley *et al.*, 2000). This study found that β-arrestin-2-GFP^2, but not β-arrestin-1-GFP^2, was recruited to endothelin receptors following ET-1 exposure using BRET^2 in HEK293 cells. β-arrestin isoforms could be functionally divergent (Srivastava *et al.*, 2015), as has been previously proposed in endothelin receptors by reports demonstrating that β-arrestin-2 knock-down prevents ET_A receptor desensitization in HEK293 cells, while β-arrestin-1 knock-down has no such effect (Morris *et al.*, 2012). On the other hand, β-arrestin-1 siRNA silencing inhibits ET-1 driven activation of Protein Kinase B (PKB) (Cianfrocca *et al.*, 2010) and MAPK signalling (Rosanò *et al.*, 2009) in the human ovarian carcinoma cell line, and prevents podocyte phenotypic changes driven by ET_A-driven signalling (Buelli *et al.*, 2013). The overall body of evidence supports that both β-arrestin isoforms are important to endothelin receptor function and my BRET^2 assays detected a constitutive β-arrestin-1 association to endothelin receptors that did not change following agonist treatment, whereas β-arrestin-2 both constitutively and dynamically associated with endothelin receptors. Thus, β-arrestin isoforms may act differentially towards endothelin physiology.

4.3 *Endothelin receptor heterodimerization inhibits β-arrestin-2 recruitment*

Through examination of $BRET_{MAX}$ values obtained by non-linear regression of BRET saturation curves obtained from β-arrestin-2-GFP^2 and Rluc-tagged endothelin receptors, I showed that co-expression of both receptor subtypes significantly decreased the extent and rate of β-arrestin-2 recruitment. Since ET-1 was used, one legitimate limitation to these experiments is that untagged endothelin receptors may be sequestering a limited pool of β-arrestin-2-GFP^2 from the opposing Rluc-tagged endothelin receptor. It is also possible that only one molecule of β-arrestin is capable of being recruited to the activated heterodimer, and thus β-arrestin-2-GFP^2 recruitment to the untagged receptor would effectively block β-arrestin-2-GFP^2 recruitment to the Rluc tagged receptor, potentially decreasing $BRET_{EFF}$. For these reasons, β-arrestin-2-GFP^2 was overexpressed at a large ratio to the endothelin receptors and an ET_B-selective agonist was tested. The ET_B-selective agonist BQ-3020 produced a similar effect to ET-1, in which case untagged ET_A did not recruit β-arrestin-2-GFP^2 to itself and must be delaying β-arrestin-2-GFP^2 recruitment to ET_B-Rluc by formation of heterodimers. This inhibition and delay in the recruitment of β-arrestin-2 would be consistent with delayed desensitization of active endothelin receptors in heterodimer, and could thus play a role in tissues co-expressing ET_A and ET_B.

4.4 *Endothelin receptor heterodimerization reduces ERK phosphorylation*

The next aim of my study was to test if ERK phosphorylation was affected by endothelin receptor heterodimerization. ERK phosphorylation downstream of endothelin receptors could ultimately be the summative result of several effectors

including PTX-sensitive Gαi, Gαq-activated PKC, and β-arrestin-dependent ERK signalling (Eishingdrelo and Kongsamut, 2013). These effectors likely contribute to ERK phosphorylation in a time-dependent fashion, as G-protein signalling is generally rapid and transient while β-arrestin signalling's onset is slower yet longer lasting (Ahn *et al.*, 2004). For this reason, Gαi, Gαq, and β-arrestin-1 inhibition were each assayed at 5 and 20 minutes after ET-1 treatment.

ET-1-driven ERK phosphorylation was found to be PTX-insensitive, suggesting endothelin receptors do not couple to Gαi. This finding would be strengthened by testing the PTX batch against a GPCR that is known to couple to Gαi such as the CB1 receptor (Shim *et al.*, 2013), as a positive control. Co-transfection with a mutant β-arrestin-1 construct that competes with endogenous β-arrestin-1 recruitment and function significantly reduced ERK phosphorylation 5 and 20 minutes after ET-1 treatment in HEK293 cells transfected with ET_A, confirming that a significant proportion of ET-1-mediated ERK phosphorylation was β-arrestin-dependent. Co-transfection with the mutant β-arrestin-1 construct also appeared to reduce ERK phosphorylation in HEK293 co-transfected with ET_A and ET_B, but failed to produce a significant effect due to large standard deviation; this should be addressed with further experimentation by increasing the number of replicates. Alternatively, this could be interpreted as a reduced importance of β-arrestin-1 dependent ERK signalling by the endothelin receptor heterodimer, which would be consistent with inhibited β-arrestin recruitment to the heterodimer.

In HEK293 cells transfected with ET_A, pre-treatment with PKC inhibitor Gö-6983 significantly reduced ERK phosphorylation at 5 minutes, but not 20 minutes,

after ET-1 treatment, consistent with a transient Gαq-dependent ERK phosphorylation. Interestingly, PKC inhibition in HEK293 cells co-transfected with both endothelin receptor subtypes appeared to also reduce ERK phosphorylation 20 minutes after ET-1 treatment, although this effect was not significant and warrants further experimentation by increasing the number of replicates. Evans and Walker (2008) conclusively demonstrated that endothelin receptor heterodimer activation induces longer lasting Ca^{2+} transients compared to homodimers. As this is a G-protein-dependent outcome of endothelin receptor activation, it can be presumed that potentially extended PKC activity would also be an effect of endothelin receptor heterodimerization. However, this could also be a consequence of synergistic signalling interactions downstream of the activation of monomeric endothelin receptors A and B. To demonstrate that the above is unequivocally tied to heterodimerization, I would have to repeat the experiments performed in this study with the non-dimerizing mutant ET_A construct (Evans and Walker, 2008). The use of this mutant ET_A construct should abolish the effects of ET_A/ET_B heterodimerization on β-arrestin recruitment and ERK phosphorylation. It would also be informative to repeat the above experiments with HEK293 cells transfected with ET_B, in order to determine if ERK activation downstream of ET_B activation is similar to ET_A-dependent ERK signalling. This is also necessary to determine if the alterations in ERK activation by co-expression of ET_A and ET_B are caused by heterodimerization or simply by expression of ET_B.

ET-1 produces a long lasting vasoconstriction in most vascular beds where both receptor subtypes are co-expressed in VSMCs (Clarke *et al.*, 1989; Macrae *et al.*, 1993; Maguire and Davenport, 2014). This could be explained by endothelin receptor heterodimerization, with previous reports highlighting that the heterodimer extends the time-frame of ET-1-induced Ca^{2+} transients in HEK293 cells and that dual antagonism of both endothelin receptors is required to block these prolonged Ca^{2+} transients (Evans and Walker, 2008). Interestingly, despite concerns pertaining to endothelial ET_B inhibition due to its importance in vasodilation, dual endothelin receptor antagonists such as bosentan have proven more clinically successful than have specific ET_A antagonists (Böhm *et al.*, 2002; Clozel and Flores, 2006; Iglarz *et al.,* 2015), which could indeed be explained by the need to antagonize both receptor subtypes when attempting to block heterodimer signaling. As such, it appears the agonist-activated heterodimer efficaciously couples to G-protein Gαq, whilst inhibiting β-arrestin-2 recruitment and signal desensitization. This would prolong signalling from activated endothelin receptors by increasing the length of time Gαq can activate PLC, leading to prolonged Ca^{2+} release and PKC activation. This is in contrast to the endothelin receptor homodimers or monomers, which are rapidly desensitized by β-arrestin recruitment and internalization (Fig. 4.1).

Figure 4.1: *Modelling endothelin receptor heterodimerization*

A. Following ET-1 binding, endothelin receptor monomers initiate Gαq-dependent Ca^{2+} release through transient PLC activation (dashed arrow) of IP_3 production and subsequent opening of IP_3-gated Ca^{2+} channels present on the endoplasmic reticulum. PLC also activates PKC through DAG production, which contributes to Ca^{2+}-independent vasoconstriction and activates numerous downstream effectors, including ERK, a regulator of gene expression that translocates to the nucleus to promote proliferation and cell-cycle progression. β-arrestin is recruited to the activated ET receptors and rapidly desensitizes the response followed by internalization, as well as directly activating ERK. **B.** Heterodimerization of ET_A and ET_B masks internalization motifs required for β-arrestin recruitment, thus prolonging the time available for the activated receptor complex to generate Ca^{2+} transients and PKC activation. Endothelin receptor heterodimerization may thus mediate the long vasoconstrictor response to ET-1 by prolonging receptor activation through inhibition of β-arrestin function.

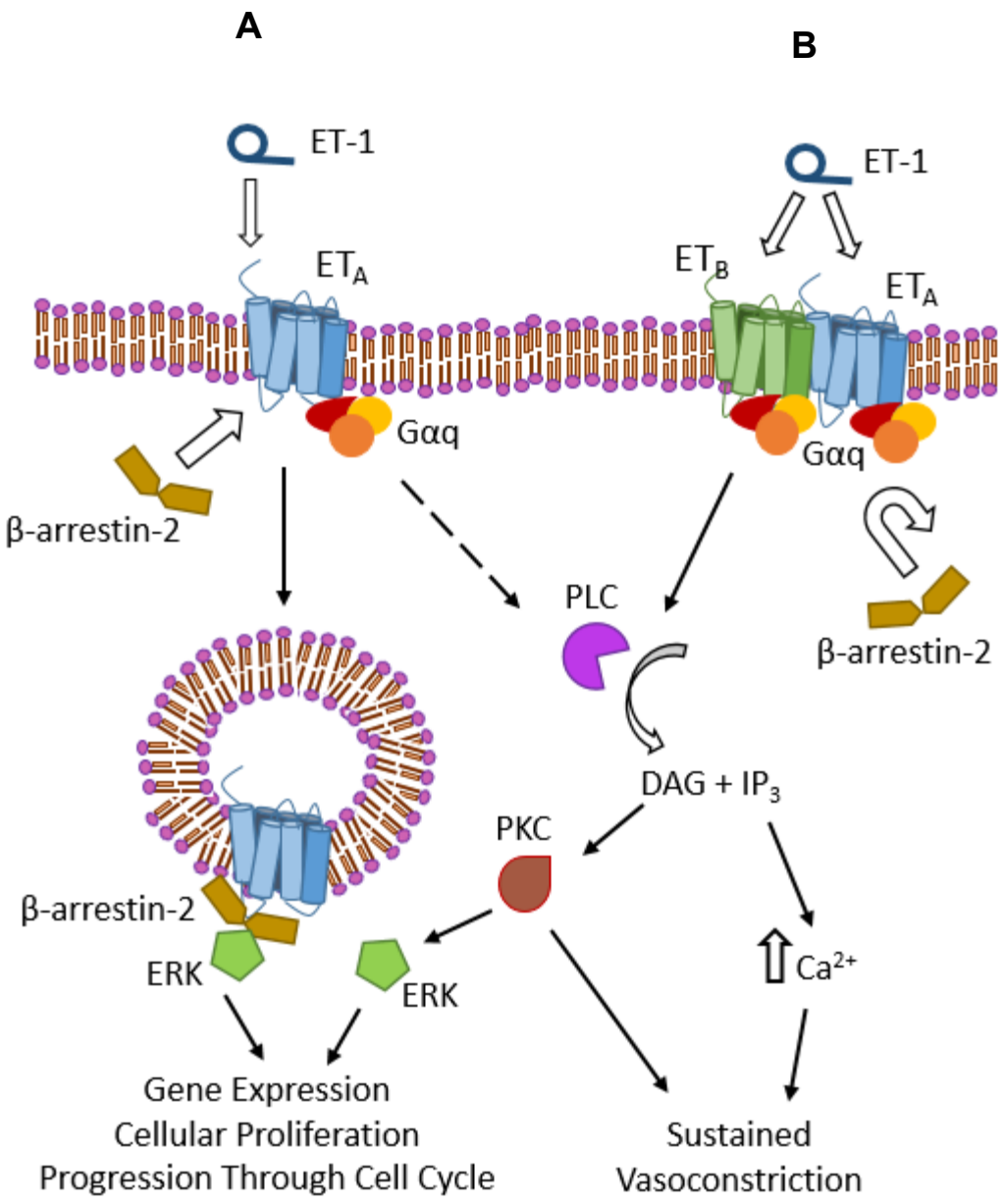
A
B
ET-1
ET-1
ET_A
ET_B
ET_A
Gαq
Gαq
β-arrestin-2
β-arrestin-2
PLC
DAG + IP_3
PKC
β-arrestin-2
ERK
ERK
Ca^{2+}
Gene Expression
Cellular Proliferation
Progression Through Cell Cycle
Sustained
Vasoconstriction

4.5 *Future directions*

As mentioned previously, the presented BRET^2 assays do not differentiate between dimers and oligomers. Recent evolutions in methodology such as sequential BRET-FRET, described in Carriba *et al.* (2008), enable the resolution of higher order GPCR complexes. Although the authors utilized this novel technique to show complexation of three separate GPCRs, it could potentially be used to detect oligomerization of endothelin receptor dimers. For example, such an assay would involve heterologous expression of ET_A-Rluc, ET_B-GFP^2, and either ET_A-YFP or ET_B-YFP. When coelenterazine induces BRET between ET_A-Rluc and ET_B-GFP^2, GFP^2 emission sequentially excites the YFP fusion protein if the third endothelin receptor is in close enough proximity for subsequent FRET. Alternatively, endothelin receptor dimers may stand alone and YFP emission would thus be unobserved.

Determining if endothelin receptor heterodimerize in tissues could be achieved using techniques such as the proximity ligation assay (described in Trifilieff *et al.,* 2011). Briefly, rolling circle DNA polymerase amplification would occur between oligonucleotide-conjugated antibodies targeting ET_A and ET_B if the antibodies were in close enough proximity. Labelled complimentary oligonucleotides would then be added to detect the cluster of amplified DNA, allowing the visualization of GPCR dimerization in native tissues. Such experimentation would either confirm or reject the premise that this interaction is physiologically relevant by providing evidence as to whether or not endothelin receptor heterodimerization occurs appreciably *in vivo*.

While my thesis was carried out using a heterologous expression system, it would be interesting to test vessel function *in situ* in a homozygous ET_B loss-of-function rat model (Gariepy *et al.*, 1998). This rodent model expresses a mutation that abrogates expression of functional ET_B. My results, along with those of previous *in vitro* reports, would predict that the endothelin receptor heterodimer increases the contractile response to ET-1 by inhibiting receptor desensitization and prolonging Ca^{2+} transients. The loss of endothelin receptor heterodimerization in vessels isolated from such animals should thus show a more transient contractile response.

Conflictingly, ET_B-deficient rats have increased systolic blood pressure compared to their wild-type counterparts (Gariepy *et al.*, 2000); this is likely explained by the loss of vasodilating endothelial ET_B, which would counteract the elimination of heterodimer signaling. This said, the ET_B loss-of-function rat model contains a deletion in exon 1 of the ET_B gene, which encodes for transmembrane helices 1 and 2, but the mutant protein is nonetheless expressed (Thakali *et al.*, 2008). This leaves open the alternative possibility that endothelin receptor heterodimerization still occurs in this transgenic model, as the domains thought to be essential to dimerization, namely the PDZ domain of ET_A and the transmembrane helix 4 of ET_B, would still yet be present (Evans and Walker, 2008). Techniques that examine GPCR dimerization natively in tissues, such as the aforementioned proximity ligation assay, could resolve this question using this model.

Tissues that co-express both receptor sub-types, such as vascular smooth muscle cells, may potentially contain a large proportion of ET_A in dimer with ET_B. Circulating ET-1 seems to be elevated with aging in humans (Miyauchi *et al.*, 1992; Fernandez-Cruz *et al.*, 1993); for this reason, vascular endothelin receptor heterodimer inhibition may be an important target in disease conditions common to the aged such as arterial hypertension and cerebral hypoperfusion. ET-1 is more important as a local paracrine factor than as a systemically circulating hormone, and is thus key to proper hemodynamics in vascular beds that rely on mechanisms of auto-regulation, such as resistance arterioles that regulate blood flow to capillaries based on the metabolic needs of surrounding tissues and are the main targetable contribution to peripheral resistance (Dunn and Nelson, 2014). It is apparent that exploring the functions of the endothelin receptor heterodimer will be important in directing endothelin-targeted clinical interventions that have thus far proven challenging (Remuzzi *et al.*, 2002) despite widespread promise in a variety of pathological conditions.

References

Ahn, S., Shenoy, S. K., Wei, H., & Lefkowitz, R. J. (2004). Differential kinetic and spatial patterns of β-arrestin and G protein-mediated ERK activation by the angiotensin II receptor. *Journal of Biological Chemistry*,*279*(34), 35518-35525.

Ahn, S., Kim, J., Hara, M. R., Ren, X. R., & Lefkowitz, R. J. (2009). β-Arrestin-2 mediates anti-apoptotic signaling through regulation of BAD phosphorylation. *Journal of Biological Chemistry*, *284*(13), 8855-8865.

Bagher, A. M., Laprairie, R. B., Kelly, M. E., & Denovan-Wright, E. M. (2013). Co-expression of the human cannabinoid receptor coding region splice variants (hCB 1) affects the function of hCB 1 receptor complexes. *European journal of pharmacology*, *721*(1), 341-354.

Bagher, A. M., Laprairie, R. B., Kelly, M. E., & Denovan-Wright, E. M. (2016). Antagonism of Dopamine Receptor 2 Long Affects Cannabinoid Receptor 1 Signaling in a Cell Culture Model of Striatal Medium Spiny Projection Neurons. *Molecular pharmacology*, *89*(6), 652-666.

Böhm, F., Ahlborg, G., Johansson, B. L., Hansson, L. O., & Pernow, J. (2002). Combined endothelin receptor blockade evokes enhanced vasodilatation in patients with atherosclerosis. *Arteriosclerosis, thrombosis, and vascular biology*, *22*(4), 674-679.

Bouvier, M., & Hébert, T. E. (2014). CrossTalk proposal: Weighing the evidence for Class A GPCR dimers, the evidence favours dimers. *The Journal of physiology*, *592*(12), 2439-2441.

Bremnes, T., Paasche, J. D., Mehlum, A., Sandberg, C., Bremnes, B., & Attramadal, H. (2000). Regulation and intracellular trafficking pathways of the endothelin receptors. *Journal of Biological Chemistry*, *275*(23), 17596-17604.

Bruchas, M. R., Macey, T. A., Lowe, J. D., & Chavkin, C. (2006). Kappa opioid receptor activation of p38 MAPK is GRK3-and arrestin-dependent in neurons and astrocytes. *Journal of Biological Chemistry*, *281*(26), 18081-18089.

Buelli, S., Rosanò, L., Gagliardini, E., Corna, D., Longaretti, L., Pezzotta, A., ... & Morigi, M. (2013). β-Arrestin-1 Drives Endothelin-1–Mediated Podocyte Activation and Sustains Renal Injury. *Journal of the American Society of Nephrology*, ASN-2013040362.

Carriba, P., Navarro, G., Ciruela, F., Ferré, S., Casadó, V., Agnati, L., ... & Lluís, C. (2008). Detection of heteromerization of more than two proteins by sequential BRET-FRET. *Nature methods*, *5*(8), 727-733.

Carvajal, J. A., Germain, A. M., Huidobro-Toro, J. P., & Weiner, C. P. (2000). Molecular mechanism of cGMP-mediated smooth muscle relaxation. *Journal of cellular physiology*, *184*(3), 409-420.

Chen, C. A., & Manning, D. R. (2001). Regulation of G proteins by covalent modification. *Oncogene*, *20*(13).

Cianfrocca, R., Rosano, L., Spinella, F., Di Castro, V., Natali, P. G., & Bagnato, A. (2010). β-arrestin-1 mediates the endothelin-1-induced activation of Akt and integrin-linked kinase. *Canadian journal of physiology and pharmacology*, *88*(8), 796-801.

Clarke, J. G., Benjamin, N. I. G. E. L., Larkin, S. W., Webb, D. J., Davies, G. J., & Maseri, A. (1989). Endothelin is a potent long-lasting vasoconstrictor in men. *American Journal of Phys.-Heart and Circulatory Phys.*, *257*(6), H2033-H2035.

Clozel, M., & Flores, S. (2006). Endothelin receptors as drug targets in chronic cardiovascular diseases: the rationale for dual antagonism. *Drug development research*, *67*(11), 825-834.

Conner, D. A., Mathier, M. A., Mortensen, R. M., Christe, M., Vatner, S. F., Seidman, C. E., & Seidman, J. G. (1997). β-Arrestin1 knockout mice appear normal but demonstrate altered cardiac responses to β-adrenergic stimulation. *Circulation research*, *81*(6), 1021-1026.

Culhane, K. J., Liu, Y., Cai, Y., & Yan, E. C. (2015). Transmembrane signal transduction by peptide hormones via family B G protein-coupled receptors. *Frontiers in pharmacology*, *6*.

Dai, X., & Galligan, J. J. (2006). Differential trafficking and desensitization of human ETA and ETB receptors expressed in HEK 293 cells. *Experimental Biology and Medicine*, *231*(6), 746-751.

Dalby, B., Cates, S., Harris, A., Ohki, E. C., Tilkins, M. L., Price, P. J., & Ciccarone, V. C. (2004). Advanced transfection with Lipofectamine 2000 reagent: primary neurons, siRNA, and high-throughput applications. *Methods*,*33*(2), 95-103.

Dalrymple, M. B., Pfleger, K. D., & Eidne, K. A. (2008). G protein-coupled receptor dimers: functional consequences, disease states and drug targets. *Pharmacology & therapeutics*, *118*(3), 359-371.

Daniels, D. J., Kulkarni, A., Xie, Z., Bhushan, R. G., & Portoghese, P. S. (2005). A bivalent ligand (KDAN-18) containing δ-antagonist and κ-agonist pharmacophores bridges δ2 and κ1 opioid receptor phenotypes. *Journal of medicinal chemistry*, *48*(6), 1713-1716.

Day, R. N., Periasamy, A., & Schaufele, F. (2001). Fluorescence resonance energy transfer microscopy of localized protein interactions in the living cell nucleus. *Methods*, *25*(1), 4-18.

Devesly, P., Phillips, P. E., Johns, A., Rubanyi, G., & Parker-Botelho, L. H. (1990). Receptor kinetics differ for endothelin-1 and endothelin-2 binding to Swiss 3T3 fibroblasts. *Biochemical and biophysical research communications*, *172*(1), 126-134.

DeWire, S. M., Ahn, S., Lefkowitz, R. J., & Shenoy, S. K. (2007). β-arrestins and cell signaling. *Annu. Rev. Physiol.*, *69*, 483-510.

DeWire, S. M., Kim, J., Whalen, E. J., Ahn, S., Chen, M., & Lefkowitz, R. J. (2008). β-arrestin-mediated signaling regulates protein synthesis. *Journal of Biological Chemistry*, *283*(16), 10611-10620.

D'Orleans-Juste, P., Plante, M., Honore, J. C., Carrier, E., & Labonte, J. (2003). Synthesis and degradation of endothelin-1. *Canadian journal of physiology and pharmacology*, *81*(6), 503-510.

Dunn, K. M., & Nelson, M. T. (2014). Neurovascular signaling in the brain and the pathological consequences of hypertension. *American Journal of Physiology-Heart and Circulatory Physiology*, *306*(1), H1-H14.

Dupré, D. J., & Hébert, T. E. (2006). Biosynthesis and trafficking of seven transmembrane receptor signalling complexes. *Cellular signalling*, *18*(10), 1549-1559.

Eglen, R. M., Bosse, R., & Reisine, T. (2007). Emerging concepts of guanine nucleotide-binding protein-coupled receptor (GPCR) function and implications for high throughput screening. *Assay and drug development technologies*,*5*(3), 425-452.

Eishingdrelo, H., & Kongsamut, S. (2013). Minireview: targeting GPCR activated ERK pathways for drug discovery. *Current chemical genomics and translational medicine*, *7*, 9-15.

Emori, T., Hirata, Y., Ohta, K., Kanno, K., Eguchi, S., Imai, T., ... & Marumo, F. (1991). Cellular mechanism of endothelin-1 release by angiotensin and vasopressin. *Hypertension*, *18*(2), 165-170.

Evans, N. J., & Walker, J. W. (2008). Sustained Ca2+ signaling and delayed internalization associated with endothelin receptor heterodimers linked through a PDZ finger *Canadian journal of physiology and pharmacology*, *86*(8), 526-535.

Fernandez-Cruz, A., Martin, P., Fernandez, L., Sanchez, J., Ibarra, J., Moya, J., ... & Otero, M. L. (1993). Plasma endothelin is increased in young essential hypertensives but not in elderly essential or diabetic hypertensives. *Journal of Hypertension*, *11*, S146-S147.

Gainetdinov, R. R., Premont, R. T., Bohn, L. M., Lefkowitz, R. J., & Caron, M. G. (2004). Desensitization of G protein-coupled receptors and neuronal functions. *Annu. Rev. Neurosci.*, *27*, 107-144.

Gandia, J., Galino, J., Amaral, O. B., Soriano, A., Lluís, C., Franco, R., & Ciruela, F. (2008). Detection of higher-order G protein-coupled receptor oligomers by a combined BRET–BiFC technique. *FEBS letters*, *582*(20), 2979-2984.

Gariepy, C. E., Williams, S. C., Richardson, J. A., Hammer, R. E., & Yanagisawa, M. (1998). Transgenic expression of the endothelin-B receptor prevents congenital intestinal aganglionosis in a rat model of Hirschsprung disease. *Journal of Clinical Investigation*, *102*(6), 1092.

Gariepy, C. E., Ohuchi, T., Williams, S. C., Richardson, J. A., & Yanagisawa, M. (2000). Salt-sensitive hypertension in endothelin-B receptor–deficient rats. *The Journal of clinical investigation*, *105*(7), 925-933.

Glass, M., Govindpani, K., Furkert, D. P., Hurst, D. P., Reggio, P. H., & Flanagan, J. U. (2016). One for the Price of Two… Are Bivalent Ligands Targeting Cannabinoid Receptor Dimers Capable of Simultaneously Binding to both Receptors? *Trends in pharmacological sciences*, *37*(5), 353-363.

Granier, S., & Kobilka, B. (2012). A new era of GPCR structural and ch1emical biology. *Nature chemical biology*, *8*(8), 670-673.

Gregan, B., Schaefer, M., Rosenthal, W., & Oksche, A. (2004). Fluorescence resonance energy transfer analysis reveals the existence of endothelin-A and endothelin-B receptor homodimers. *Journal of cardiovascular pharmacology*, *44*, S30-S33.

Gurevich, V. V., & Gurevich, E. V. (2008). GPCR monomers and oligomers: it takes all kinds. *Trends in neurosciences*, *31*(2), 74-81.

Harding, P. J., Attrill, H., Boehringer, J., Ross, S., Wadhams, G. H., Smith, E., ... & Watts, A. (2009). Constitutive dimerization of the G-protein coupled receptor, neurotensin receptor 1, reconstituted into phospholipid bilayers. *Biophysical journal*, *96*(3), 964-973.

Hillion, J., Canals, M., Torvinen, M., Casadó, V., Scott, R., Terasmaa, A., ... & Canela, E. I. (2002). Coaggregation, Cointernalization, and Codesensitization of Adenosine A2A Receptors and Dopamine D2 Receptors. *Journal of Biological Chemistry*, *277*(20), 18091-18097.

Iglarz, M., Steiner, P., Wanner, D., Rey, M., Hess, P., & Clozel, M. (2015). Vascular Effects of Endothelin Receptor Antagonists Depends on Their Selectivity for ETA Versus ETB Receptors and on the Functionality of Endothelial ETB Receptors. *Journal of cardiovascular pharmacology*, *66*(4), 332.

Ihara, M., Saeki, T., Fukuroda, T., Kimura, S., Ozaki, S., Patel, A. C., & Yano, M. (1992). A novel radioligand [125I] BQ-3020 selective for endothelin (ETB) receptors. *Life sciences*, *51*(6), PL47-PL52.

Katritch, V., Cherezov, V., & Stevens, R. C. (2013). Structure-function of the G-protein-coupled receptor superfamily. *Annual review of pharmacology and toxicology*, *53*, 531.

Kaupmann, K., Malitschek, B., Schuler, V., Heid, J., Froestl, W., Beck, P., ... & Karschin, A. (1998). GABAB-receptor subtypes assemble into functional heteromeric complexes. *Nature*, *396*(6712), 683-687.

Kerppola, T. K. (2008). Bimolecular fluorescence complementation (BiFC) analysis as a probe of protein interactions in living cells. *Annual review of biophysics*, *37*, 465.

Kido, T., Sawamura, T., & Masaki, T. (1998). The processing pathway of endothelin-1 production. *Journal of cardiovascular pharmacology*, *31*, S13-S15.

Kim, J., Ahn, S., Rajagopal, K., & Lefkowitz, R. J. (2009). Independent β-arrestin2 and Gq/protein kinase Cζ pathways for ERK stimulated by angiotensin type 1A receptors in vascular smooth muscle cells converge on transactivation of the epidermal growth factor receptor. *Journal of Biological Chemistry*, *284*(18), 11953-11962.

Kohout, T. A., Lin, F. T., Perry, S. J., Conner, D. A., & Lefkowitz, R. J. (2001). β-Arrestin 1 and 2 differentially regulate heptahelical receptor signaling and trafficking. *Proceedings of the National Academy of Sciences*,*98*(4), 1601-1606.

Lefkowitz, R. J., & Shenoy, S. K. (2005). Transduction of receptor signals by ß-arrestins. *Science*, *308*(5721), 512-517.

Ling, L., Maguire, J. J., & Davenport, A. P. (2013). Endothelin-2, the forgotten isoform: emerging role in the cardiovascular system, ovarian development, immunology and cancer. *British journal of pharmacology*,*168*(2), 283-295.

Lovell, K. M., Frankowski, K. J., Stahl, E. L., Slauson, S. R., Yoo, E., Prisinzano, T. E., ... & Bohn, L. M. (2015). Structure–Activity Relationship Studies of Functionally Selective Kappa Opioid Receptor Agonists that Modulate ERK 1/2 Phosphorylation While Preserving G Protein Over βArrestin2 Signaling Bias. *ACS chemical neuroscience*, *6*(8), 1411-1419.

Luttrell, L. M., Roudabush, F. L., Choy, E. W., Miller, W. E., Field, M. E., Pierce, K. L., & Lefkowitz, R. J. (2001). Activation and targeting of extracellular signal-regulated kinases by β-arrestin scaffolds. *Proceedings of the National Academy of Sciences*, *98*(5), 2449-2454.

Luttrell, L. M., & Lefkowitz, R. J. (2002). The role of β-arrestins in the termination and transduction of G-protein-coupled receptor signals. *Journal of cell science*, *115*(3), 455-465.

Macrae, I. M., Robinson, M. J., Graham, D. I., Reid, J. L., & McCulloch, J. (1993). Endothelin-1-induced reductions in cerebral blood flow: dose dependency, time course, and neuropathological consequences. *Journal of Cerebral Blood Flow & Metabolism*, *13*(2), 276-284.

Maguire, J. J., & Davenport, A. P. (2014). Endothelin@ 25–new agonists, antagonists, inhibitors and emerging research frontiers: IUPHAR Review 12. *British journal of pharmacology*, *171*(24), 5555-5572.

Martins, S. A., Trabuco, J. R., Monteiro, G. A., Chu, V., Conde, J. P., & Prazeres, D. M. F. (2012). Towards the miniaturization of GPCR-based live-cell screening assays. *Trends in biotechnology*, *30*(11), 566-574.

McDonald, P. H., Chow, C. W., Miller, W. E., Laporte, S. A., Field, M. E., Lin, F. T., ... & Lefkowitz, R. J. (2000). β-Arrestin 2: a receptor-regulated MAPK scaffold for the activation of JNK3. *Science*, *290*(5496), 1574-1577.

Milligan, G., Canals, M., Pediani, J. D., Ellis, J., & Lopez-Gimenez, J. F. (2007). The role of GPCR dimerisation/oligomerisation in receptor signalling. In *GPCRs: From Deorphanization to Lead Structure Identification* (pp. 145-162). Springer Berlin Heidelberg.

Miyauchi, T., Yanagisawa, M., Iida, K., Ajisaka, R., Suzuki, N., Fujino, M., ... & Sugishita, Y. (1992). Age-and sex-related variation of plasma endothelin-1 concentration in normal and hypertensive subjects. *American heart journal*, *123*(4), 1092-1093.

Moaven, H., Koike, Y., Jao, C. C., Gurevich, V. V., Langen, R., & Chen, J. (2013). Visual arrestin interaction with clathrin adaptor AP-2 regulates photoreceptor survival in the vertebrate retina. *Proceedings of the National Academy of Sciences*, *110*(23), 9463-9468.

Morris, G. E., Nelson, C. P., Brighton, P. J., Standen, N. B., Challiss, R. J., & Willets, J. M. (2012). Arrestins 2 and 3 differentially regulate ETA and P2Y2 receptor-mediated cell signaling and migration in arterial smooth muscle. *American Journal of Physiology-Cell Physiology*, *302*(5), C723-C734.

Oakley, R. H., Laporte, S. A., Holt, J. A., Caron, M. G., & Barak, L. S. (2000). Differential affinities of visual arrestin, βarrestin1, and βarrestin2 for G protein-coupled receptors delineate two major classes of receptors. *Journal of Biological Chemistry*, *275*(22), 17201-17210.

Oldham, W. M., & Hamm, H. E. (2008). Heterotrimeric G protein activation by G-protein-coupled receptors. *Nature Reviews Molecular Cell Biology*, *9*(1), 60-71.

Pearson, G., Robinson, F., Beers Gibson, T., Xu, B. E., Karandikar, M., Berman, K., & Cobb, M. H. (2001). Mitogen-activated protein (MAP) kinase pathways: regulation and physiological functions 1. *Endocrine reviews*, *22*(2), 153-183.

Petkov, G. V. (2012). Role of potassium ion channels in detrusor smooth muscle function and dysfunction. *Nature Reviews Urology*, *9*(1), 30-40.

Pfleger, K. D., & Eidne, K. A. (2003). New technologies: bioluminescence resonance energy transfer (BRET) for the detection of real time interactions involving G-protein coupled receptors. *Pituitary*, *6*(3), 141-151.

Pfleger, K. D., & Eidne, K. A. (2006). Illuminating insights into protein-protein interactions using bioluminescence resonance energy transfer (BRET). *Nature methods*, *3*(3), 165-174.

Pfleger, K. D., Seeber, R. M., & Eidne, K. A. (2006). Bioluminescence resonance energy transfer (BRET) for the real-time detection of protein-protein interactions. *Nature Protocols*, *1*(1), 337.

Pierce, K. L., & Lefkowitz, R. J. (2001). Classical and new roles of β-arrestins in the regulation of G-protein-coupled receptors. *Nature reviews neuroscience*, *2*(10), 727-733.

Preininger, A. M., Meiler, J., & Hamm, H. E. (2013). Conformational flexibility and structural dynamics in GPCR-mediated G protein activation: a perspective. *Journal of molecular biology*, *425*(13), 2288-2298.

Remuzzi, G., Perico, N., & Benigni, A. (2002). New therapeutics that antagonize endothelin: promises and frustrations. *Nature Reviews Drug Discovery*, *1*(12), 986-1001.

Richer, M., David, M., Villeneuve, L. R., Trieu, P., Ethier, N., Pétrin, D., ... & Hébert, T. E. (2009). GABA-B1 Receptors are Coupled to the ERK1/2 MAP Kinase Pathway in the Absence of GABA-B2 Subunits. *Journal of molecular neuroscience*, *38*(1), 67-79.

Rosanò, L., Cianfrocca, R., Masi, S., Spinella, F., Di Castro, V., Biroccio, A., ... & Bagnato, A. (2009). β-Arrestin links endothelin A receptor to β-catenin signaling to induce ovarian cancer cell invasion and metastasis. *Proceedings of the National Academy of Sciences*, *106*(8), 2806-2811.

Ross, E. M. (2013). G protein GTPase-activating proteins: regulation of speed, amplitude, and signaling selectivity. In *Recent Progress in Hormone Research-Volume 50: Proceedings of the 1993 Laurentian Hormone Conference* (p. 207). Academic Press.

Shenoy, S. K., Drake, M. T., Nelson, C. D., Houtz, D. A., Xiao, K., Madabushi, S., ... & Lefkowitz, R. J. (2006). β-Arrestin-dependent, G protein-independent ERK1/2 activation by the β2 adrenergic receptor. *Journal of Biological Chemistry*, *281*(2), 1261-1273.

Shim, J. Y., Ahn, K. H., & Kendall, D. A. (2013). Molecular Basis of Cannabinoid CB1 Receptor Coupling to the G Protein Heterotrimer Gαiβγg. *Journal of Biological Chemistry*, *288*(45), 32449-32465.

Smith, J. S., & Rajagopal, S. (2016). The β-arrestins: Multifunctional regulators of G protein-coupled receptors. *Journal of Biological Chemistry*,*291*(17), 8969-8977.

Srivastava, A., Gupta, B., Gupta, C., & Shukla, A. K. (2015). Emerging functional divergence of β-arrestin isoforms in GPCR function. *Trends in Endocrinology & Metabolism*, *26*(11), 628-642.

Svoboda, P., Teisinger, J., Novotny, J., Bourova, L., Drmota, T., Hejnova, L., ... & Vokurkova, A. (2004). Biochemistry of transmembrane signaling mediated by trimeric G proteins. *Physiological research*, *53*, S141-152.

Terrillon, S., & Bouvier, M. (2004). Roles of G-protein-coupled receptor dimerization. *EMBO reports*, *5*(1), 30-34.

Thakali, K., Galligan, J. J., Fink, G. D., Gariepy, C. E., & Watts, S. W. (2008). Pharmacological endothelin receptor interaction does not occur in veins from ETB receptor deficient rats. *Vascular pharmacology*, *49*(1), 6-13.

Tohgo, A., Pierce, K. L., Choy, E. W., Lefkowitz, R. J., & Luttrell, L. M. (2002). β-Arrestin scaffolding of the ERK cascade enhances cytosolic ERK activity but inhibits ERK-mediated transcription following angiotensin AT1a receptor stimulation. *Journal of Biological Chemistry*, *277*(11), 9429-9436.

Tostes, R. C., Fortes, Z. B., Callera, G. E., Montezano, A. C., Touyz, R. M., Webb, R. C., & Carvalho, M. H. C. (2008). Endothelin, sex and hypertension. *Clinical Science*, *114*(2), 85-97.

Trifilieff, P., Rives, M. L., Urizar, E., Piskorowski, R. A., Vishwasrao, H. D., Castrillon, J., ... & Javitch, J. A. (2011). Detection of antigen interactions ex vivo by proximity ligation assay: endogenous dopamine D2-adenosine A2A receptor complexes in the striatum. *Biotechniques*, *51*(2), 111.

Venkatakrishnan, A. J., Deupi, X., Lebon, G., Tate, C. G., Schertler, G. F., & Babu, M. M. (2013). Molecular signatures of G-protein-coupled receptors. *Nature*, *494*(7436), 185-194.

Villemure, J. F., Lynda, A. D. A. M., Bevan, N. J., Gearing, K., Chenier, S., & Bouvier, M. (2005). Subcellular distribution of GABAB receptor homo-and hetero-dimers. *Biochemical Journal*, *388*(1), 47-55.

Vozzi, F., Bianchi, F., Ahluwalia, A., & Domenici, C. (2014). Hydrostatic pressure and shear stress affect endothelin-1 and nitric oxide release by endothelial cells in bioreactors. *Biotechnology journal*, *9*(1), 146-154.

Webb, R. C. (2003). Smooth muscle contraction and relaxation. *Advances in physiology education*, *27*(4), 201-206.

Whorton, M. R., Bokoch, M. P., Rasmussen, S. G., Huang, B., Zare, R. N., Kobilka, B., & Sunahara, R. K. (2007). A monomeric G protein-coupled receptor isolated in a high-density lipoprotein particle efficiently activates its G protein. *Proceedings of the National Academy of Sciences*, *104*(18), 7682-7687.

Yanagisawa, M., Kurihara, H., Kimura, S., Tomobe, Y., Kobayashi, M., Mitsui, Y., ... & Masaki, T. (1988). A novel potent vasoconstrictor peptide produced by vascular endothelial cells. *Nature*, *332*(6163), 411-415.

Zhang, X. C., Liu, J., & Jiang, D. (2014). Why is dimerization essential for class-C GPCR function? New insights from mGluR1 crystal structure analysis. *Protein & cell*, *5*(7), 492.

Appendix I

License for Figure 1.2

ELSEVIER LICENSE
TERMS AND CONDITIONS

Jul 28, 2016

This Agreement between Adel Zrein ("You") and Elsevier ("Elsevier") consists of your license details and the terms and conditions provided by Elsevier and Copyright Clearance Center.

License Number	3917650633190
License date	Jul 28, 2016
Licensed Content Publisher	Elsevier
Licensed Content Publication	Trends in Biotechnology
Licensed Content Title	Towards the miniaturization of GPCR-based live-cell screening assays
Licensed Content Author	Sofia A.M. Martins,João R.C. Trabuco,Gabriel A. Monteiro,Virginia Chu,João P. Conde,D. Miguel F. Prazeres
Licensed Content Date	November 2012
Licensed Content Volume Number	30
Licensed Content Issue Number	11
Licensed Content Pages	9
Start Page	566
End Page	574
Type of Use	reuse in a thesis/dissertation
Portion	figures/tables/illustrations
Number of figures/tables/illustrations	1
Format	print
Are you the author of this Elsevier article?	No
Will you be translating?	No
Order reference number	
Original figure numbers	1
Title of your thesis/dissertation	Endothelin Receptor Heterodimerization Inhibits β-arrestin Function
Expected completion date	Aug 2016
Estimated size (number of pages)	80
Elsevier VAT number	GB 494 6272 12
Requestor Location	Adel Zrein 5850 College St Room 6-E1 Halifax, NS B3H 4H7 Canada Attn: Adel Zrein
Total	0.00 CAD

Appendix II

License for Figure 1.3

JOHN WILEY AND SONS LICENSE TERMS AND CONDITIONS

Jul 26, 2016

This Agreement between Adel Zrein ("You") and John Wiley and Sons ("John Wiley and Sons") consists of your license details and the terms and conditions provided by John Wiley and Sons and Copyright Clearance Center.

License Number	3915980035011
License date	Jul 25, 2016
Licensed Content Publisher	John Wiley and Sons
Licensed Content Publication	EMBO Reports
Licensed Content Title	Roles of G-protein-coupled receptor dimerization
Licensed Content Author	Sonia Terrillon,Michel Bouvier
Licensed Content Date	Jan 1, 2004
Licensed Content Pages	5
Type of use	Dissertation/Thesis
Requestor type	University/Academic
Format	Print
Portion	Figure/table
Number of figures/tables	1
Original Wiley figure/table number(s)	Figure 1
Will you be translating?	No
Title of your thesis / dissertation	Endothelin Receptor Heterodimerization Inhibits β-arrestin Function
Expected completion date	Aug 2016
Expected size (number of pages)	80
Requestor Location	Adel Zrein 5850 College St Room 6-E1 Halifax, NS B3H 4H7 Canada Attn: Adel Zrein
Publisher Tax ID	EU826007151
Billing Type	Invoice
Billing Address	Adel Zrein 5850 College St Room 6-E1 Halifax, NS B3H 4H7 Canada Attn: Adel Zrein
Total	0.00 CAD